ARC Centre of Excellence in Population Ageing Research

Working Paper 2020/23

Subnational old-age mortality modeling: Accounting for underreporting in a Bayesian framework

Qian Lu, Katja Hanewald, Andres M. Villegas and Xiaojun Wang

Subnational old-age mortality modeling: Accounting for underreporting in a Bayesian framework

Qian Lu[a,c], Katja Hanewald[b,c], Andrés M. Villegas[b,c], Xiaojun Wang[d,*]

[a] *School of Statistics, Renmin University of China, Beijing 100872, China*
[b] *School of Risk and Actuarial Studies, UNSW Sydney, New South Wales 2052, Australia*
[c] *CEPAR, UNSW Sydney, New South Wales 2052, Australia*
[d] *Center for Applied Statistics of Renmin University of China, Beijing 100872, China*

Abstract

Accurate old-age mortality projections for subnational areas are important for assessing health outcomes and valuing pension liabilities. However, subnational mortality data often face small sample sizes at older ages. In some countries, the underreporting of deaths and population numbers poses additional problems. We propose a new Bayesian framework for old-age mortality that allows for death underreporting by introducing a reporting probability, which is defined as the ratio of reported deaths to real deaths and uses informative priors derived from demographic death distribution methods. We show that the proposed modeling framework works well for province-level old-age mortality data (ages 60–99) in China over 1982–2010. Compared to a more conventional framework that assumes the reported data are accurate and uses reported mortality data directly, the proposed framework provides a better fit, with a lower deviance information criterion. The proposed framework generates a reasonable mortality curvature and coherent forecasts for subpopulations with sparse or incomplete mortality data.

Keywords: Old-age mortality, Subnational modeling, Bayesian framework, Death underreporting

JEL: G22, J11

1. Introduction

Mortality improvements at older ages translate into longer life expectancy and population aging worldwide (Gavrilov et al., 2017). Therefore, accurate mortality projections for older ages are important for actuaries and the policymakers concerned with the design and reforms of pension systems. However, within one country, the lifespans often have large regional inequalities and high variabilities at older ages (e.g., Permanyer and Scholl, 2019). As such, decisions based

*Corresponding author
Email address: xiaojun_wang@ruc.edu.cn (Xiaojun Wang)

on national mortality forecasts will overlook subnational heterogeneity and potentially lead to overly simplistic conclusions on longevity (Permanyer and Scholl, 2019). Moreover, accurate subnational mortality projections for older ages are particularly important for countries with decentralized pension funds, such as the United States, where most pension plans are sponsored by local governments (Gale and Krupkin, 2016).

One challenge to modeling the mortality at older ages is the relatively poor data quality. Even in developed countries where the vital registration is high quality (Cairns et al., 2016; Peralta et al., 2020), there are potential errors and significant anomalies in the number of exposure-to-risk (Cairns et al., 2016). Additionally, as the sample size of older ages is smaller than that of middle ages, especially in subnational areas, the registered mortality data for older ages can be subject to volatility, incomplete death reporting, and misreporting, having sparse or no observations in the death counts at advanced ages (Leknes and Løkken, 2020; Schmertmann and Gonzaga, 2018). Thus, for older ages, the registered mortality data are often inaccurate in developed countries, leading to spurious patterns of mortality deceleration and plateaus (Gavrilov and Gavrilova, 2019a, 2019b). In countries without reliable vital registration records, censuses are the main source of mortality data. However, census mortality data can also suffer from incomplete death reporting, which leads to data unreliability (Hill, 2009; Peralta et al., 2020). Therefore, for both developed and developing countries, it is important to account for underreported data and small sample sizes when projecting future subnational mortality rates for older ages.

Death underreporting is also a problem in the reports of the Coronavirus disease (COVID-19) and, thus, requires new modeling solutions. Due to the COVID-19 outbreak, medical resources are limited in many countries, and the deaths related to COVID-19 reported by hospitals are likely to be underreported or accounted as other causes of death (Jagodnik et al., 2020). These issues provide additional motivation for our research.

We propose to use a Bayesian framework to study the impact of underreported deaths on the modeling of old-age mortality. The proposed framework introduces the reporting probability to account for underreported deaths, defined as the ratio of reported deaths to real deaths. The reporting probability uses informative priors derived from demographic death distribution methods, while the proposed mortality model in the framework is based on the Cairns–Blake–Dowd (CBD) model family (Cairns et al., 2006, 2009) with normalized age function. Our results show that death underreporting cannot be overlooked because it affects both the model fit and mortality forecasts.

We use a death distribution method called the generalized growth balance method to esti-

mate the priors for the reporting probability. Death distribution methods are widely used in the demographic literature to evaluate the coverage of registered deaths in census data (e.g., Hill, 2004, 2009; Queiroz et al., 2017; Peralta et al., 2020). Three main death distribution methods are commonly employed: the generalized growth balance (GGB) method, the synthetic extinct generations (SEG) method, and the combined GGB-SEG method (Hill, 2009). We use the generalized growth balance method in this paper. Under this method, data from a baseline census are used to estimate the coverage of deaths in another census.

Building on an emerging literature, we use a Bayesian framework to cope with inaccurate mortality data. Cairns et al. (2016) study the errors in exposures and propose a model in a Bayesian framework to quantify the errors in exposures for England and Wales using data from the Office of National Statistics (ONS). Alexander et al. (2017) emphasize the advantage of the Bayesian framework in dealing with missing data and use it to estimate the subnational mortality in the United States and France. Schmertmann and Gonzaga (2018) combine death distribution methods with the Bayesian framework in mortality modeling to analyze Brazil subnational mortality in 2010.

The mortality model in our framework is based on the CBD family of mortality models with normalized age function. The CBD family of mortality models is designed specifically for post-age-60 (Cairns et al., 2006, 2009), being recently extended to a multi-population setting by Li et al. (2015) and Li and Liu (2019) with common factors for males and females using high-quality mortality data for developed countries. The CBD family uses period effects and a parametric age function to project the mortality for any age, even outside the age range of the sample data (Dowd and Blake, 2019). Therefore, the CBD family is useful to model the mortality at advanced ages when data quality is poor. Although we use a model variant of the CBD family to study old-age mortality, our proposed underreporting modeling framework is not constrained to one specific mortality model, and the CBD-type model we use could be replaced by any other alternative model form.

We apply the framework to the provincial mortality in China for the age range 60–99 over 1982–2010. Previous demographic research shows that Chinese population data are of good quality (e.g., Banister and Hill, 2004; Coale and Li, 1991), whereas census deaths in China suffer from underreporting (e.g., Wang, 2003; Wang and Ge, 2013). We model the unobserved real mortality rates and the observed reported mortality rates together and then compare the impact of the underreported deaths on the modeling of old-age mortality. This relatively new dataset for China has only been used by Lu et al. (2019), who developed Bayesian hierarchical mortality models for all ages, without underreporting.

Compared with previous studies, such as Li and Liu (2019) and Schmertmann and Gonzaga (2018), our framework considers the problem of inaccurate mortality data and produces reasonable projections. Compared with a version of the model without underreporting, which assumes the data are accurate and models the registered mortality directly, the proposed model has better performance, with a lower value of the deviance information criterion (DIC), and produces more reasonable mortality curves despite the volatile data. The model also performs well in projections and generates coherent forecasts.

We contribute two main aspects to the literature. First, we consider the reporting probability in mortality modeling, which is useful to countries with unreliable mortality datasets. As mortality data at advanced ages have sparse observations, which are potentially underreported, our study provides a new solution to modeling advanced-age mortality. Second, our framework yields a novel coherent model to estimate and forecast subnational mortality. The model works well for sub-populations, where mortality rates have substantial variations in historical levels and trends.

Our study shows that there can be important differences in the estimated and projected mortality results with and without accounting for underreporting. Problematic mortality forecasts and conclusions can be derived if underreporting is ignored, which can have severe consequences for the pension system and insurance companies. Hence, further studies on mortality modeling should account for incomplete reporting, where the reporting probability can also be useful in cause-of-death mortality modeling. Moreover, as the reported deaths due to COVID-19 are likely to be underreported, researchers should analyze the mortality due to COVID-19 with caution. While we do not explore the application of our methods to the modeling of COVID-19 mortality in this paper, our proposed framework offers a possible approach for accounting the underreporting of COVID-19 deaths.

The remainder of the paper is structured as follows. Section 2 introduces the proposed model. Section 3 describes the mortality database. Section 4 presents and compares the fitting results of the proposed model with a similar model without underreporting. Section 5 presents the forecasting performance of the proposed model and the model without underreporting. Section 6 provides conclusions and ideas for future research.

2. Model

2.1. Model summary

We propose a new mortality model under a Bayesian framework to estimate and forecast old-age mortality rates at the subnational level. The model explicitly accounts for underreporting.

The statistical approach is summarized in Figure 1.

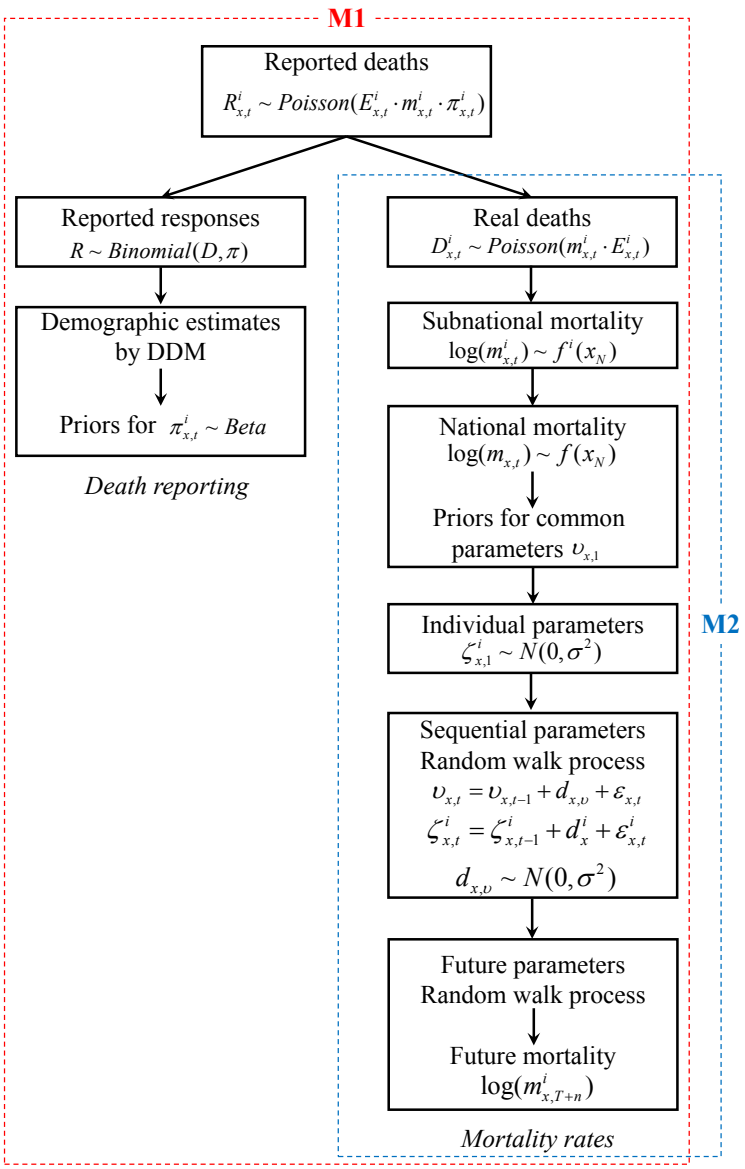

Figure 1. Proposed framework

The real number of age-specific deaths, $D^i_{x,t}$, is defined as the unobserved real number of deaths at age x in year t for sub-population i, while the reported number of deaths, $R^i_{x,t}$, is defined as the observed number from census or registration data. The reported deaths follow a Poisson distribution with the mean equal to the product of the observed age-specific exposures $E^i_{x,t}$, the mortality rates $m^i_{x,t}$, and the reporting probabilities $\pi^i_{x,t}$. Additionally, the reported deaths follow a Binomial distribution with the "number of experiments" given by the real deaths and the "success probability" by the reporting probability. The reporting probability is modeled using information estimated by death distribution methods as priors for a beta distribution.

Under the proposed framework, denoted as M1 in Figure 1, the real deaths follow a Poisson distribution of the exposures and unobserved real mortality rates. The real mortality is modeled

using a parametric model that has common and individual parameters for subnational areas. The initial values of the common parameters use prior information, estimated by the national mortality of the reference year (i.e., the year with the best-quality data). The initial values of the individual parameters follow normal distributions. The subsequent and future parameters are modeled using a random walk process. The future mortality rates are forecasted based on the parameter forecasts.

To show the impact of the reporting probability on mortality estimation and projection, we compare M1 with a version of the framework without the reporting probability, denoted as M2 in Figure 1. Under M2, the reported data are assumed to be accurate and the reported deaths are used as real deaths (i.e., $R^i_{x,t} = D^i_{x,t}$) to model mortality.

2.2. Detailed model description

We adopt a Bayesian framework, where the real number of deaths, $D^i_{x,t}$, is assumed to be conditionally independent and follow a Poisson distribution:

$$D^i_{x,t} \sim Poisson(E^i_{x,t} \cdot m^i_{x,t}), \tag{1}$$

where $E^i_{x,t}$ is the number of age-specific exposures for sub-population i and $m^i_{x,t}$ the central death rate for people aged x at year t in sub-population i.

To account for incomplete death reporting, we follow an approach similar to that of Schmertmann and Gonzaga (2018) and introduce an age-specific reporting probability, $\pi^i_{x,t}$, for people aged x at year t in sub-population i. We use death distribution methods to estimate the priors for $\pi^i_{x,t}$. The reported number of deaths, $R^i_{x,t}$, is modeled independently for each age and year from a binomial distribution:

$$R^i_{x,t} \sim Binomial(D^i_{x,t}, \pi^i_{x,t}). \tag{2}$$

The age-specific reporting probability, $\pi^i_{x,t}$, is modeled independently for each age and year from a beta distribution, which is a conjugated prior for the binomial distribution:

$$\pi^i_{x,t} \sim Beta(K_t\phi_t, K_t[1-\phi_t]), \tag{3}$$

where K_t and ϕ_t are the priori shape and scale parameters of the beta distribution, computed by the estimates of death distribution methods described in Section 3. The mean and variance of the estimates derived by death distribution methods are denoted as μ_t and s^2_t, respectively. The shape and scale parameters are respectively computed as $\phi_t = \mu_t$ and $K_t = \frac{\mu_t(1-\mu_t)}{s^2_t} - 1$ (Glen and Leemis, 2017; Schmertmann and Gonzaga, 2018).

Schmertmann and Gonzaga (2018) prove that the marginal distribution of the joint Poisson and binomial process has a Poisson likelihood. This means $R^i_{x,t}$ still follows a Poisson distribution:

$$R^i_{x,t} \sim Poisson(E^i_{x,t} \cdot m^i_{x,t} \cdot \pi^i_{x,t}). \tag{4}$$

As the CBD model family performs well in advanced-age mortality modeling when data quality is not optimal, we propose a general model form based on the CBD family to model the subnational mortality $m^i_{x,t}$. However, we note that the proposed underreporting modeling framework is independent of the specification of the model for $m^i_{x,t}$ and the CBD-type model could be replaced by other alternative model. For example, instead of using the CBD approach discussed here, we could overlay the subnational Bayesian approach presented by Alexander et al. (2017) or any other appropriate method for modeling subnational mortality at older ages.

To avoid possible numerical problems caused by the different scales of age/period terms (Hunt and Blake, 2020), we use the normalized age functions in our specification of the mortality for the subnational populations:

$$log(m^i_{x,t}) = a_t x^2_N + b_t x_N + c_t + g^i_t x_N + h^i_t + \epsilon^i_{x,t}, \tag{5}$$

where $m^i_{x,t}$ is the central mortality rate at age x in year t ($t = t_1, t_2, ..., t_T$, where t_T is the last year in the sample range) for sub-population i. In Equation (5), $x_N = \frac{x-\bar{x}}{x-x_{min}} \in [0, 1]$ is the normalized age function, with x_{min} denoting the minimum age in the sample range; a_t, b_t, and c_t are the common parameters among all sub-populations; g^i_t and h^i_t are individual parameters for sub-population i; and $\epsilon^i_{x,t}$ is a random error drawn from a normal distribution, $N(0, \sigma^2_\epsilon)$.

We use a random walk process to model the time-dependent parameters in $m^i_{x,t}$. To obtain the estimation and projection in one stage, we draw the initial values of the parameters ($t = t_1$) from normal distributions.

We assume that there is a "best year" of mortality data, where underreporting is lowest, and reporting is highest compared among all data available. We denote this year as the reference year. In practice, the reference year can be chosen either based on the information on reporting quality from literature or from the estimates of the death distribution methods with the highest coverage. In this paper, we take the first approach and estimate the national mortality data in the reference year. The estimated information of the national mortality is used as priors for the initial values of the common parameters. Thus, a_t, b_t, and c_t are respectively modeled from the following informative priors:

$$a_{t_1} \sim N(\mu_a, \sigma^2_a), b_{t_1} \sim N(\mu_b, \sigma^2_b), c_{t_1} \sim N(\mu_c, \sigma^2_c), \tag{6}$$

where μ_a, μ_b, and μ_c are the parameters computed by fitting the national mortality data of the reference year.

The initial values of the individual parameters are modeled from the following non-informative priors:

$$g^i_{t_1} \sim N(0, \sigma^2_{g^i}), h^i_{t_1} \sim N(0, \sigma^2_{h^i}), \tag{7}$$

where σ^2_a, ..., $\sigma^2_{h^i}$, σ^2_ϵ are the variances from inverse gamma (IG) distributions, for example, $\sigma^2_a \sim IG(1, 0.01)$.

The subsequent values of parameters at time $t = t_2, ..., t_T$ are modeled by a random walk process:

$$a_{t_m} \sim N(a_{t_{m-1}} + \Delta_m \cdot d_a, \Delta_m \cdot \sigma^2_{\epsilon a}), \tag{8}$$

$$b_{t_m} \sim N(b_{t_{m-1}} + \Delta_m \cdot d_b, \Delta_m \cdot \sigma^2_{\epsilon b}), \tag{9}$$

$$c_{t_m} \sim N(c_{t_{m-1}} + \Delta_m \cdot d_c, \Delta_m \cdot \sigma^2_{\epsilon c}), \tag{10}$$

$$g^i_{t_m} \sim N(g^i_{t_{m-1}} + \Delta_m \cdot d^i_g, \Delta_m \cdot \sigma^2_{\epsilon g^i}), \tag{11}$$

$$h^i_{t_m} \sim N(h^i_{t_{m-1}} + \Delta_m \cdot d^i_h, \Delta_m \cdot \sigma^2_{\epsilon h^i}), \tag{12}$$

where $\Delta_m = t_m - t_{m-1}$ denotes the year gap between times t_m and t_{m-1} ($m = 1, 2, ..., T$). That is, our model allows for data to be collected at irregular time intervals (rather than annually). Variances $\sigma^2_{\epsilon a}, ..., \sigma^2_{\epsilon h^i}$ are independently modeled from $IG(1, 0.01)$. The drifts $d_a, ..., d^i_h$ are from non-informative priors:

$$d_a \sim N(0, \sigma^2_{d_a}), d_b \sim N(0, \sigma^2_{d_b}), d_c \sim N(0, \sigma^2_{d_c}), d^i_g \sim N(0, \sigma^2_{d_g}), d^i_h \sim N(0, \sigma^2_{d_h}), \tag{13}$$

where the variances $\sigma^2_{d_a}, ..., \sigma^2_{d_h}$ are from $IG(1, 0.01)$. The drifts d^i_g and d^i_h are modeled from the same prior distributions, $N(0, \sigma^2_{d_g})$ and $N(0, \sigma^2_{d_h})$, to pool information among provinces.

The future parameters are also forecasted by a random walk process. For example, a_{t_T+n} is forecasted as:

$$a_{t_T+n} = a_{t_T+n-1} + d_a + \zeta_a, \tag{14}$$

where n is the number of years ahead to forecast and ζ_a is the random error drawn from the posterior normal distribution $N(0, \sigma^2_{\zeta a})$, with $\sigma^2_{\zeta a} = \sigma^2_{\epsilon a}$. Other parameters are forecasted similarly to a_{t_T+n}.

The simulated trajectories of the future mortality rates in year $t_T + n$ are then obtained by:

$$log(m^i_{x,t_T+n}) = a_{t_T+n} x^2_N + b_{t_T+n} x_N + c_{t_T+n} + g^i_{t_T+n} x_N + h^i_{t_T+n}. \tag{15}$$

3. Data

We use province-level census data from four censuses conducted in China in 1982, 1990, 2000, and 2010 ($t = t_1, t_2, t_3, t_4$, respectively). The data contain the population and death counts by gender and age for every available province. Except for the census data in 1990, which have 90+ as the open-ended age in the death data for all provinces, the other censuses have deaths and population data up to age 100+ for most provinces. As previously mentioned, this underexplored dataset has only been used by Lu et al. (2019), who compiled it based on data from the archive of the National Bureau of Statistics of China.

While the quality of Chinese mortality data is sometimes questioned, previous studies show that population data from China are of reasonable quality for adult ages (e.g., Banister and Hill, 2004; Coale, 1984; Coale and Banister, 1994). Death counts for the 1982 census, which was conducted under the guidance of the United Nations, are also widely considered accurate (e.g., Li, 1994; Sun et al., 1993; Zhai, 1989). However, there is evidence of underreporting of deaths in the 1990, 2000, and 2010 censuses, the estimated underreporting ratios ranging between 8.55% and 27.1%, as shown in Table 1 (e.g., Cui et al., 2013; Li, 1994; Wang, 2003).

Table 1. Underreporting estimates in previous studies

Year	1982	1990	2000	2010
Death underreporting	small	8.55% – 17%	10% – 15%	13.6% – 27.1%
Refernces	Zhai (1989)	Li (1994), Sun et al. (1993)	Wang (2003)	Cui et al. (2013)

Coale and Li (1991) conclude that old-age mortality and population data in most Chinese provinces are accurate. This is because Han Chinese, who are the main ethnic group in China, use the lunar calendar and animal years (zodiacs) to remember their birthdays. A noteworthy exception where the accuracy of the data may be problematic is Xinjiang Province, which has a Muslim majority. Based on the findings of Coale and Li (1991), we use the data for males from all available provinces except Xinjiang, and gather the data by single year of age from age 60 to 99. For the provinces without available death and population data up to 99+ years old, we use the highest ages (below the open age interval) available and treat the data for the ages above 99 as missing data. The number of exposure-to-risk is approximated by the Coale and Demeny formula (Coale et al., 1983; Preston et al., 2000) based on the census population data.

We do not account for migration in our model. Although there is rural-urban migration in China, the migration rates at older ages are low. During 2000–2010, migrants above age 60 constituted only around 5% of all migrants, and less than 2% of people aged 65+ years

old migrated (Ma et al., 2014; Zou and Wu, 2013). We thus ignore migration and use death distribution methods.

Since the data in 1982 are widely considered accurate in the literature (e.g., Zhai, 1989; Sun et al., 1993; Li, 1994), we use 1982 as the reference year and estimate the values for 1990, 2000, and 2010. We estimate the prior values of K_t and ϕ_t in 1990, 2000, and 2010 ($t = t_m$; $m \geq 2$; $t_1 = 1982, ..., t_4 = 2010$) by the generalized growth balance of the death distribution methods (Hill, 2009) using the DDM R package (Riffe et al., 2017). We calculate the death distribution methods estimates for every province and use the average mean and variance of these provincial estimates as priors for μ_t and s_t^2. Table 2 reports these priors for years 1990, 2000, and 2010.

Table 2. Priors for μ_t and s_t^2 during 1990–2010

Year	1990	2000	2010
μ_t	0.8961	0.8264	0.9023
s_t^2	0.0113	0.0293	0.0352

The death distribution method only estimates the death coverage for the censuses after 1982. Hence, we need to make assumptions on the death coverage in 1982. Based on the information that data in 1982 are accurate (e.g., Li, 1994; Sun et al., 1993; Zhai, 1989), we assume that: (1) the mean of the reporting probability in 1982 is higher than that in other years and (2) the variance of the reporting probability in 1982 is smaller than the average variance in other years. To capture these assumptions, we model the mean and variance of the death distribution estimate in 1982 using the following uniform distributions:

$$\mu_{t_1} \sim U(\mu_{max}, 1), s_{t_1}^2 \sim U(0, \bar{s}^2), \tag{16}$$

where μ_{max} is the highest μ_t in 1990, 2000, and 2010, and $\bar{s}^2$ is the mean of s_t^2 in 1990, 2000, and 2010 ($t = t_m$; $m \geq 2$).

4. Estimation results

In this section, we apply the proposed model (M1) to China's provinces and compare it with the version without underreporting (model M2). Recall from Section 2.1 that M2 is similar to M1, except that we replace Equation (4) with assumption $R_{x,t}^i = D_{x,t}^i$.

The posterior distributions are obtained using the rjags R package (Plummer, 2019), which generates samples via the Markov Chain Monte Carlo (MCMC) algorithm using Gibbs sampling. For models M1 and M2, we generate two chains and thin the chains at every 10th

observation. The Gibbs sampling converges within 10,000 iterations. After a burn-in of 20,000 iterations and convergence tests, the posterior distributions are estimated based on the last 20,000 recorded samples.

4.1. Estimated parameters

The performances of M1 and M2 are evaluated by the DIC. The DIC is a Bayesian extension of the Akaike information criterion (AIC) and a popular model selection criterion to deal with informative priors in Bayesian hierarchical models (Yan et al., 2018). A lower DIC value indicates a better model fit, and a DIC difference of 3–5 is considered significant (Khana et al., 2018). The DIC is 45,704.7 for M1 and 46,151.9 for M2, which means the model fit improves significantly by incorporating the reporting probability.

The estimated a_t, b_t, and c_t for M1 and M2 are shown in Figure 2. The white lines show the estimated medians and the areas shaded in grey the 95% posterior intervals for M1. The black lines and dashed lines show the estimated medians and the corresponding 95% posterior intervals for M2, respectively. Parameter a_t captures the age curvature of the mortality curves. The same prior for a_{t_1} makes the posterior a_{t_1} similar for M1 and M2. However, the subsequent a_t ($t = t_m$; $m \geq 2$) vary because of the reporting probability $\pi^i_{x,t}$. Using $\pi^i_{x,t}$ to correct for incomplete deaths, M1 has a more stable a_t, indicating that the curvature of age is gradually changing over time. The age curvature in M2 changes more significantly than in M1, implying M2 recognizes the data incompleteness as a pattern of the mortality profile. As for b_t and c_t, M1 yields a similar trend to M2, but with lower values. Further, M1 gives narrower intervals for b_t and wider intervals for c_t.

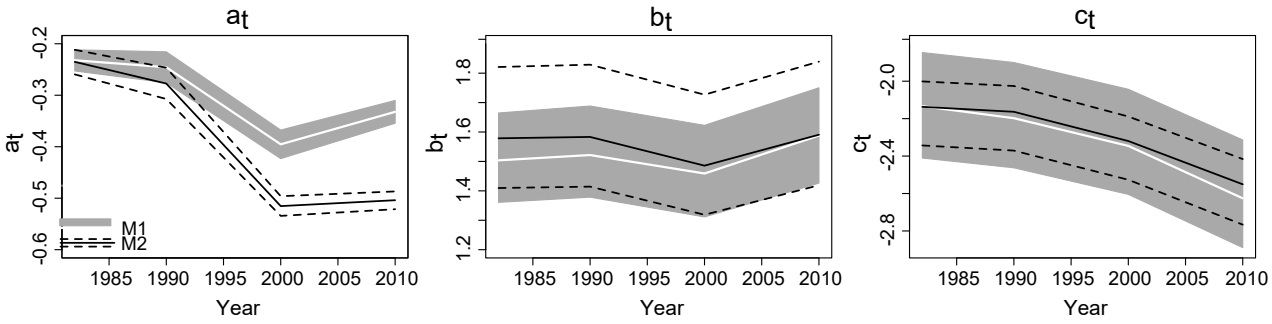

Figure 2. Estimated parameters for M1 and M2: Posterior medians and the 95% intervals of parameters a_t, b_t, and c_t

The medians of g^i_t and h^i_t in models M1 and M2 are shown in Figures 3 and 4, respectively. The dark grey lines and grey shadings respectively show the medians and 95% posterior intervals for M1. The black lines and dashed lines show the estimated medians and corresponding 95%

posterior intervals for M2. In agreement with the lower values of b_t and c_t in M1, M1 has higher posterior distributions of g_t^i and h_t^i than M2 during 1982–2010 for most provinces, except for Shanxi Province in 2000. M1 has narrower posterior intervals of g_t^i and wider posterior intervals of h_t^i, which are in line with the interval widths of b_t and c_t in Figure 2. The results for Shanxi Province are due to data errors, which we will discuss in detail later. In 1990, the intervals of g_t^i and h_t^i in both models for Chongqing Province stand out as being the widest ones. This is because Chongqing is the only province with missing data in 1990. Data for Chongqing Province are also missing in 1982, which also result in wider intervals for g_t^i and h_t^i in this year.

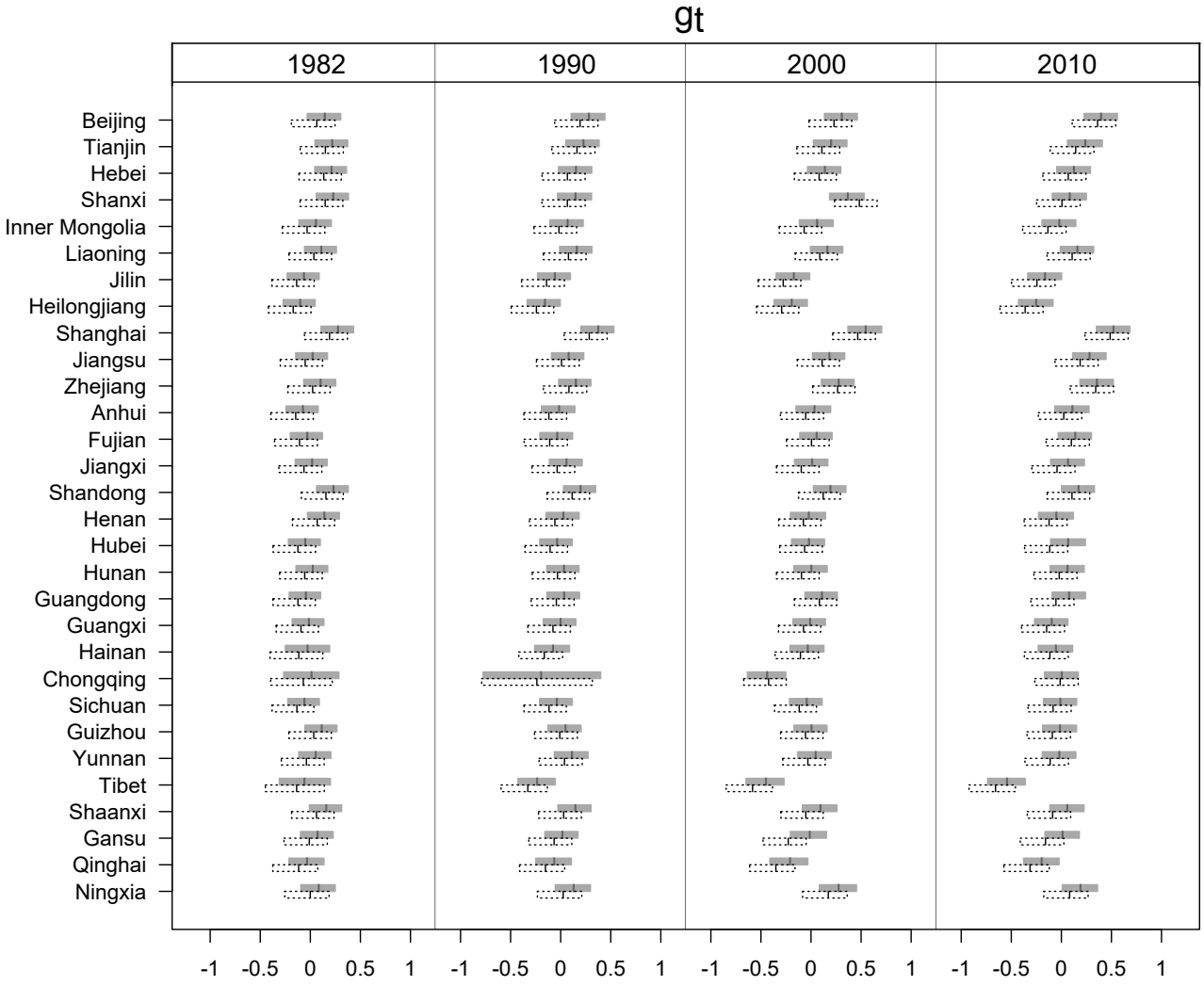

Figure 3. Estimated parameters for M1 and M2: Posterior medians and 95% intervals for g_t^i

4.2. Estimated reporting probability

The posterior medians of reporting probability $\pi_{x,t}^i$ for every age in M1 are shown in Figure 5. Each colored line represents a province. The thicker black dashed line is the national average of all provinces, denoted as $\pi_{x,t}^C$. The posterior medians are flat for some ages due to missing

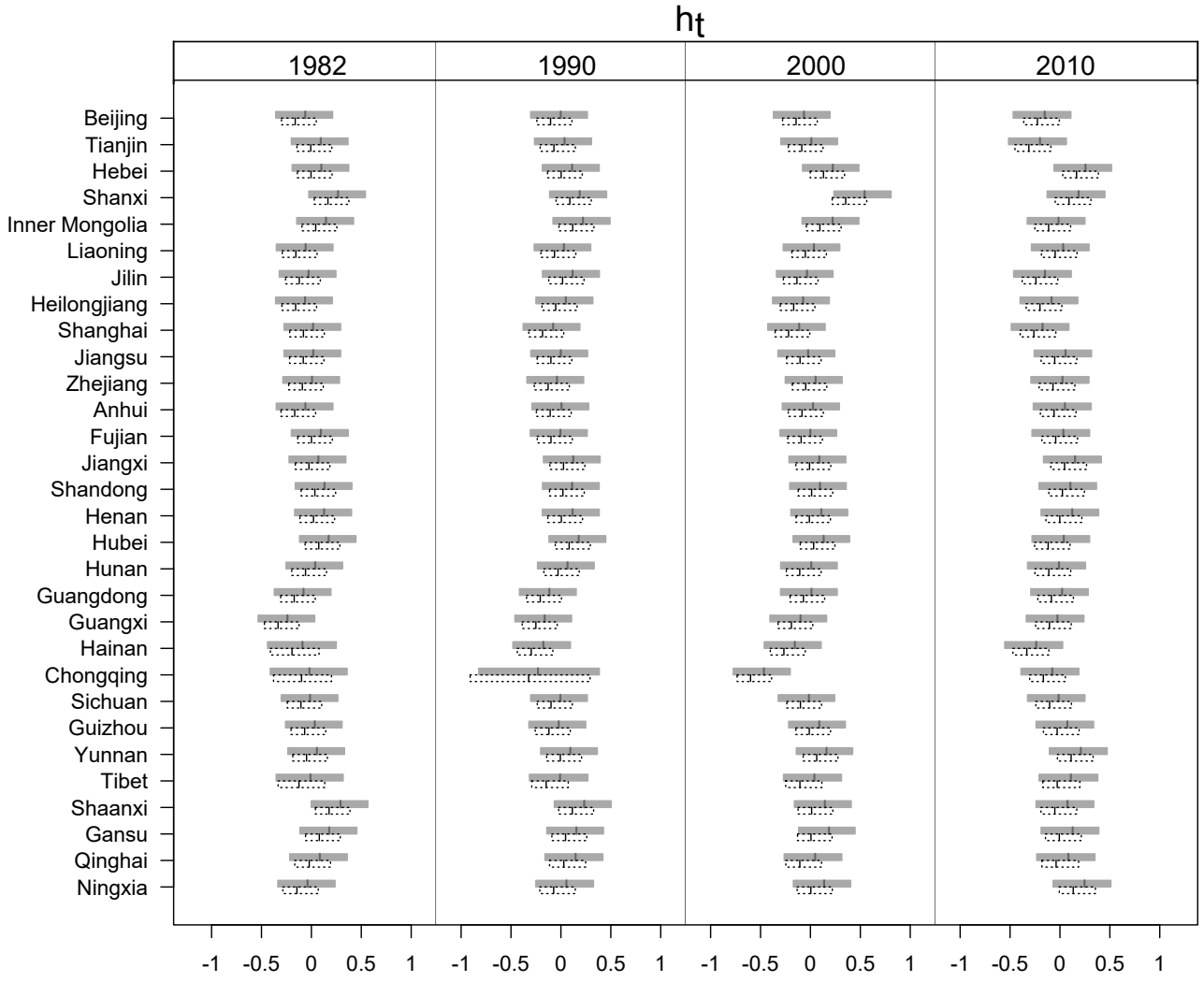

Figure 4. Estimated parameters for M1 and M2: Posterior medians and 95% intervals for h_t^i

data. The death distribution methods estimate the death coverage for data in five-year-old age groups (Hill, 2009); however, if the death coverage for a single age needs to be estimated, our model can be used as an alternative.

For 1982 and 1990, reporting probability $\pi_{x,t}^i$ fluctuates around $\pi_{x,t}^C$ and has no obvious age trend. The national average reporting ratios for all ages are 91.3% and 93.6% in 1982 and 1990, respectively. However, in 2000 and 2010, $\pi_{x,t}^i$ decreases above age 90 and has a clear trend. The national average reporting ratios under age 90 are 91.4% and 96.3% in 2000 and 2010, respectively. The national average reporting ratios above age 95 are only 71.1% and 70.8% in 2000 and 2010, while the minimum values of $\pi_{x,t}^i$ in 2000 and 2010 are estimated as 24.7% and 20.8%, respectively. The lower reporting probability for 90+ years old indicates underreporting could be severe for the oldest ages in China, which is consistent with reports from developed countries (Gavrilov and Gavrilova, 2019a).

To compare the differences in the posterior intervals between older and younger ages, we

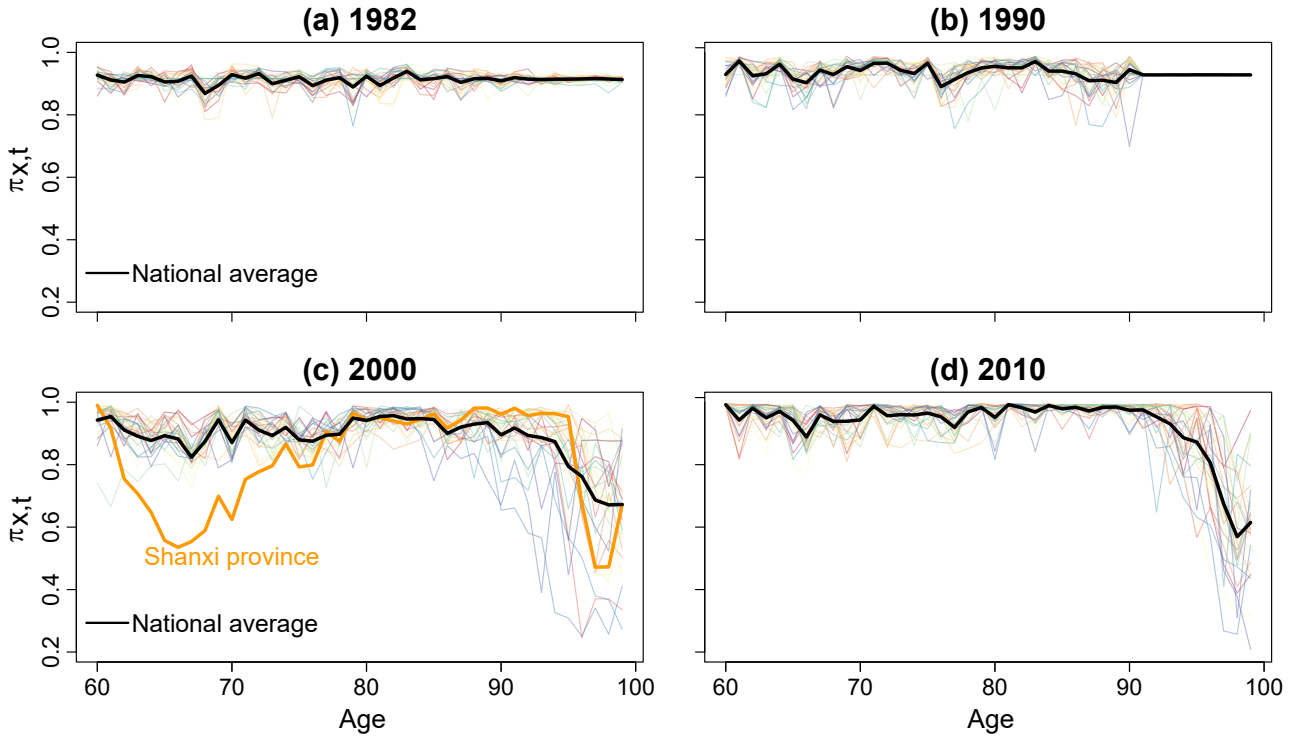

Figure 5. Posterior median of provincial reporting probability $\pi^i_{x,t}$ in M1

show the 95% posterior intervals of $\pi^i_{x,t}$ at ages 60, 90, and 95 in 2000 and 2010 ($\pi^i_{60,t}$, $\pi^i_{90,t}$, and $\pi^i_{95,t}$; $t = t_3$ and t_4) in Figure 6. The dark grey lines and grey shaded areas show the medians and the 95% posterior intervals for M1. Overall, the order of the widths of the posterior intervals is $\pi^i_{95,t} > \pi^i_{90,t} > \pi^i_{60,t}$, reflecting larger uncertainties at older ages. Between 2000 and 2010, the uncertainty is larger in 2000, indicating census data are more volatile in 2000. In provinces such as Anhui, the larger posterior intervals occur at ages 90 and 95 (red rectangles) due to missing data above age 90. However, the larger posterior intervals of less economically developed provinces such as Tibet and Qinghai (blue rectangles) are because of the small populations and volatile reported deaths at advanced ages. The posterior intervals of $\pi^i_{x,t}$ show that missing or volatile reported data result in larger reporting probability uncertainty.

The outlier reporting probability for Shanxi in Figure 5(c) is due to reported data errors. Figure 7(a) shows Shanxi's posterior medians of $\pi^i_{x,t}$ in 2000, which are the same as in Figure 5(c). Figure 7(b) shows the reported mortality and estimated median mortality for Shanxi and other provinces in 2000. The orange points and line in Figure 7(b) are the reported and estimated mortality rates of Shanxi, respectively. The grey points in Figure 7(b) are the reported mortality rates of other provinces. The S-shaped reported mortality rates of Shanxi show systematic errors in 2000: under age 75, the mortality rates are abnormally low compared to age 60, while the reported mortality rates above age 75 are unusually high compared to other provinces. As the estimation results are based on reported data, the lower reported mortality

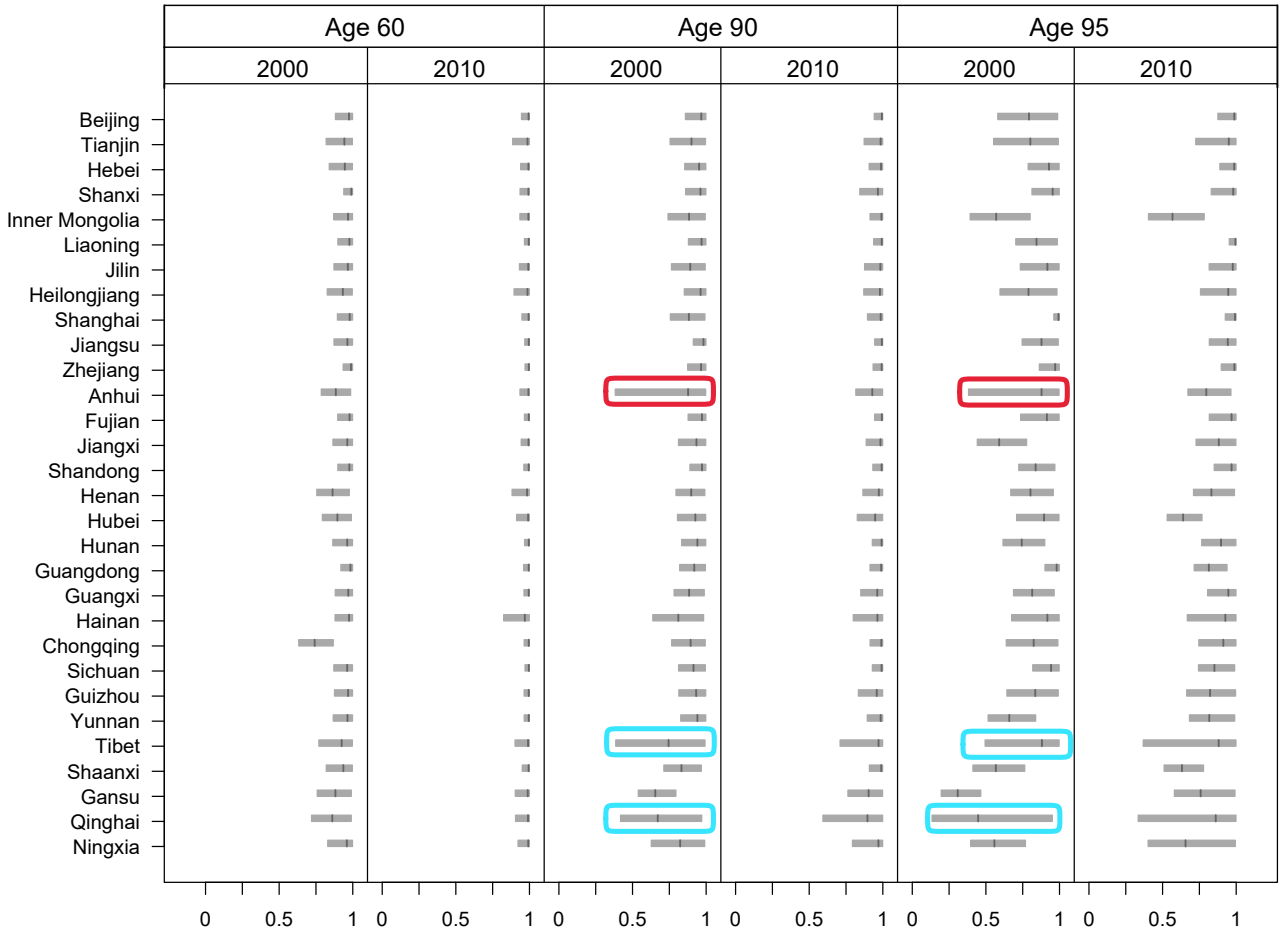

Figure 6. 95% posterior intervals of provincial reporting probability $\pi^i_{x,t}$ at ages 60, 90, and 95 in 2000 and 2010 for M1

under age 75, together with higher reported mortality above age 75, result in the extremely low reporting probability under age 75 for Shanxi Province.

4.3. Estimated mortality rates

Figure 8 shows the posterior medians of real mortality $log(m^i_{x,t})$ and registered mortality $log(r^i_{x,t})$ for ages 60–99. From Equation (4), we have $log(r^i_{x,t}) = log(m^i_{x,t} \cdot \pi^i_{x,t})$. As there are 160 curves for $log(m^i_{x,t})$ and $log(r^i_{x,t})$, respectively, for the 40 age group and four time points (1982, 1990, 2000, and 2010), we show three provinces representing eastern, central, and western China (Beijing, Henan, Gansu) in Figure 8. In China, life expectancy is closely related to economic development (see, e.g., Zhou et al., 2016). Eastern China is the most economically developed and has a longer life expectancy, while western China is least developed and has a shorter life expectancy (Zhou et al., 2016). Comparisons of other provinces can be found in the Appendix.

The black dots in Figure 8 are the historical registered data, the black lines are fitted real mortality $log(m^i_{x,t})$ for model M2, the red lines are fitted real log mortality rates $log(m^i_{x,t})$ for model M1, and the cyan dashed lines are fitted registered log mortality rates $log(r^i_{x,t})$ for

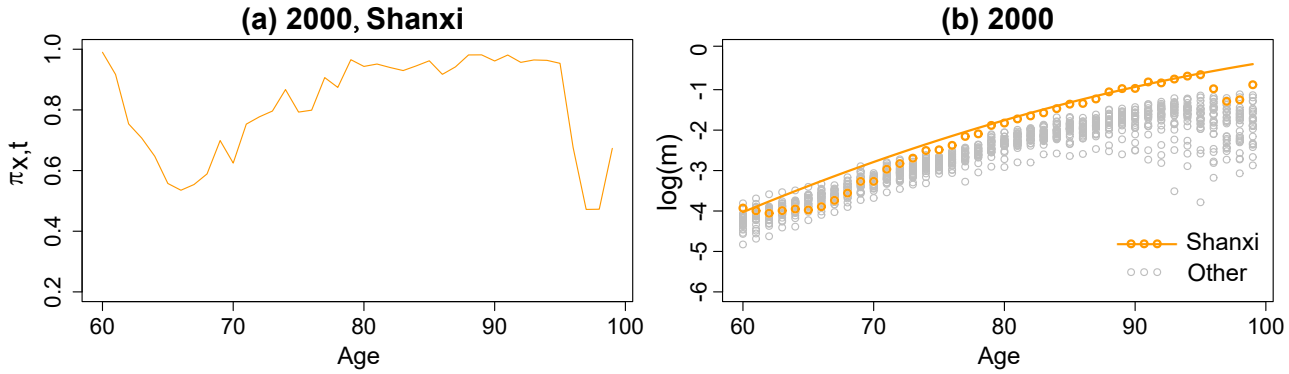

Figure 7. $\pi^i_{x,t}$ for Shanxi and reported mortality for all provinces in 2000 (estimated mortality of Shanxi is shown as orange line)

M1. Using the reporting probability $\pi^i_{x,t}$ to correct for death underreporting, M1 gives higher estimates of real mortality $log(m^i_{x,t})$ than M2, and registered mortality $log(r^i_{x,t})$ in M1 fluctuates around $log(m^i_{x,t})$ in M2. When the reporting probability $\pi^i_{x,t}$ is higher, as in 1982 and 1990 (in the first two rows in Figure 8), the estimations of the real mortality rates are not significantly impacted, the results being close for M1 and M2.

When $\pi^i_{x,t}$ is lower, as for age 90+ in 2000 and 2010 (in the last two rows in Figure 8), the real mortality for M1 is much higher than that for M2. As a result, the age curvatures of the fitted real mortality at age 90+ are markedly different between M1 and M2, which confirms the different evolution of a_t in Figure 2. Therefore, the comparison between younger ages (under age 75) and older ages (above age 90) yields a similar conclusion: the estimations of real mortality are not significantly impacted when there is good reporting. However, if there is substantial underreporting, the impact of real mortality on the estimations can be significant.

For age 60, underreporting does not make a significant difference when compared to age 95 because of good reporting. Similarly, the results for the years 1982 and 2010 suggest good reporting. However, when there is underreporting, the impact is significant. It is important to note that, in a model without the reporting probability, missing and underreporting data will dominate the mortality curves at higher ages, leading to unusual age curvatures and underestimation of real mortality. Therefore, without the reporting probability, mortality modeling for advanced ages might give incorrect mortality profiles. Based on these results, conclusions for mortality plateaus at advanced ages should be questioned because the deceleration of mortality at advanced ages can result from death underreporting.

Figure 9 shows the posterior medians and 95% intervals based on model M1 for Beijing, Henan, and Gansu in 1982 and 2010. The black dots are the reported mortality rates, while the red lines and pink intervals are the posterior medians and 95% intervals, respectively.

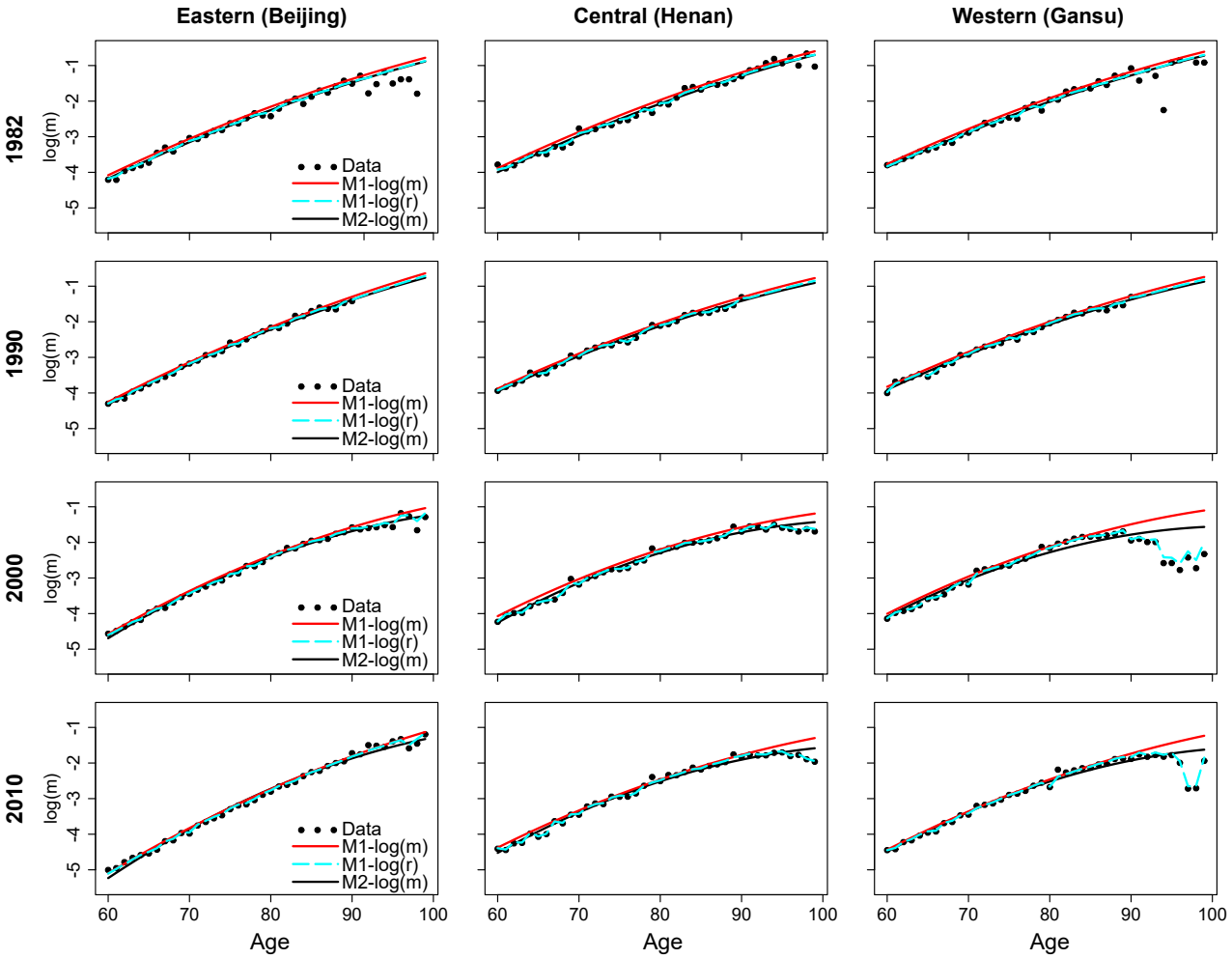

Figure 8. Posterior medians for real and registered mortality for M1 and M2

The comparison between 1982 and 2010 shows that more volatile reported data produce wider intervals due to the larger historical uncertainties. The comparison of younger and older ages, for example under age 70 with above age 90, shows that more underreported data also result in wider intervals. The posterior intervals of other provinces are provided in the Appendix.

A key feature of the Bayesian framework is that it can naturally deal with missing data. In our dataset, the death counts for Tibet are missing in 1982. Figure 10 shows the posterior median and 95% interval for Tibet in 1982 and 2010 based on model M1. In 1982, the mortality rate has a wider interval than that in 2010, which is the result of larger uncertainty due to missing data.

5. Forecasting performance

In the previous section, we showed the importance of reporting probability $\pi^i_{x,t}$ for the estimation. In the following, we present forecasts with and without $\pi^i_{x,t}$.

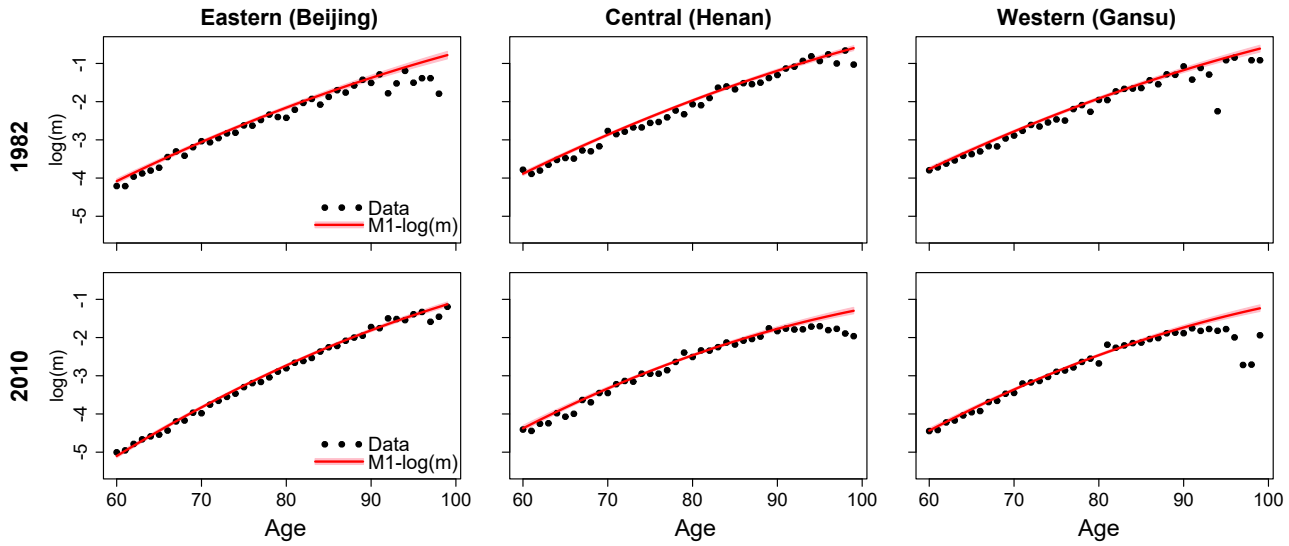

Figure 9. Posterior medians and 95% intervals for M1 in 2010 (Gansu, Henan, and Beijing)

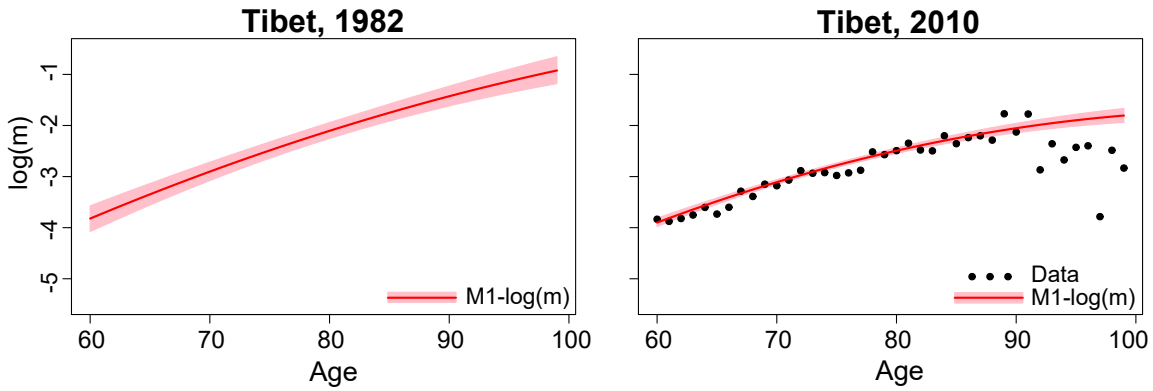

Figure 10. Posterior medians and 95% intervals for Tibet based on M1

5.1. Median mortality forecasts

Using M1 and M2, we forecast real mortality $log(m^i_{x,t})$ for 20 years, up to 2030. The forecasts for 2020 and 2030 are shown in Figure 11. The red and black lines are the forecasts for M1 and M2, respectively. Similar to the fittings, the forecasts for M1 and M2 have different age curvatures. The $log(m^i_{x,t})$ forecasts of M2 are lower for ages 60–65 and above age 85. The model without reporting probability underestimates mortality at advanced ages (above 85). Compared to 2020 (the first row in Figure 11), the difference is larger in 2030 (the second row in Figure 11), which indicates that the difference between the M1 and M2 forecasts will increase with the forecasting years. Furthermore, across provinces (across the columns in Figure 11), the differences in forecasts are larger for the less developed western provinces than for the more developed eastern provinces. As the mortality data at advanced ages are more volatile in Gansu, as shown in Figure 8, the underestimation will be more severe when data quality is not so good. Therefore, modeling without the reporting probability will underestimate the fit, as

well as the forecasts, resulting in a possibly spurious mortality plateau at advanced ages.

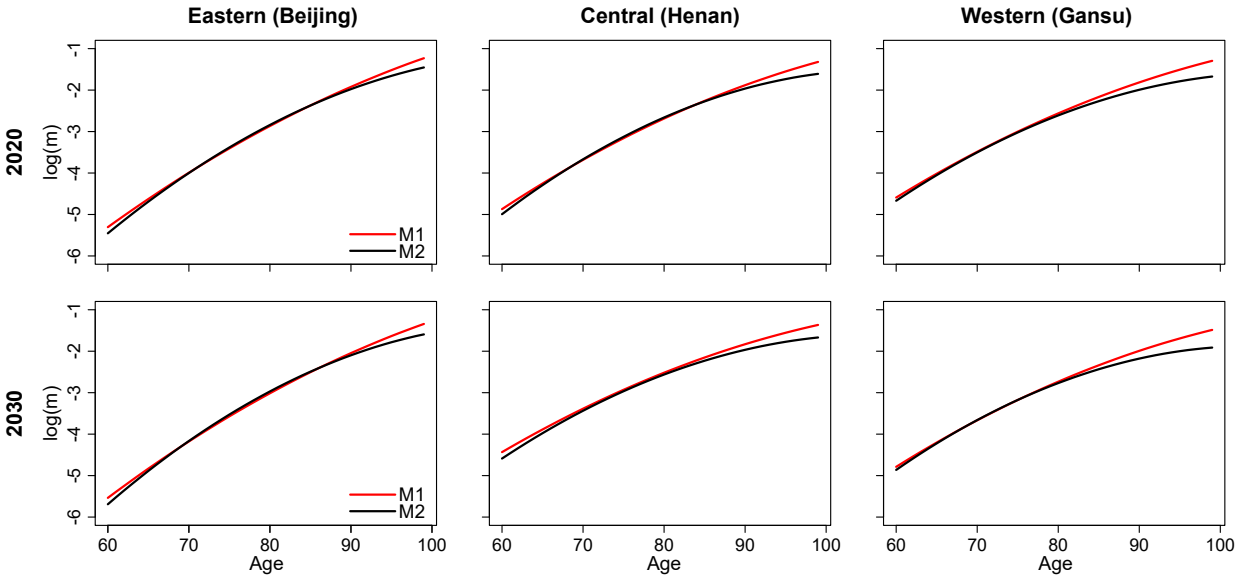

Figure 11. Median forecasts of $log(m^i_{x,t})$ for M1 and M2 in 2020 and 2030

Figure 12 shows the forecasts of $log(m^i_{x,t})$ for M1 over 2011–2030 for three selected provinces. The results for the other provinces are available in the Appendix. The first and second rows show the forecasts by age and year, respectively. Compared with historical trends, we also show the fits for 1982–2010 in Figure 12. Each shaded blue line in the first row represents a year, and darker shaded lines represent later years; each shaded blue line in the second row represents a one-year age group, and darker shaded lines represent higher ages. The dashed lines are the estimates and the solid lines the corresponding forecasts. For different provinces, the forecasts over 2011–2030 maintain the historical pattern, decreasing more rapidly at some ages as a result of the different mortality improvements over 1982–2010. For example, the forecasts for ages 60–70 decrease more rapidly than those for higher ages in Beijing because of the higher mortality improvement at lower ages during 1982–2010. In Henan and Gansu, the forecasts decrease evenly at all ages, which is plausible based on the historical trends in Gansu.

The forecasts for model M1 are coherent among provinces. Figure 13 shows the median estimations and forecasts of $log(m^i_{x,t})$ for M1 at ages 65 and 95 for all provinces, where the dashed lines are the estimations, the solid lines the forecasts, and each colored line represents a province. Although provinces have different historical mortality profiles, for a specific age, the mortality forecasts for M1 are coherent among all provinces.

Figure 14 shows the forecasts for Shanxi Province, which has outlier reporting probabilities and mortality estimations due to the unusual reported mortality data in 2000. Each shaded blue line in Figure 14(a) represents a year, and each (dashed) blue line in Figure 14(b) represents an

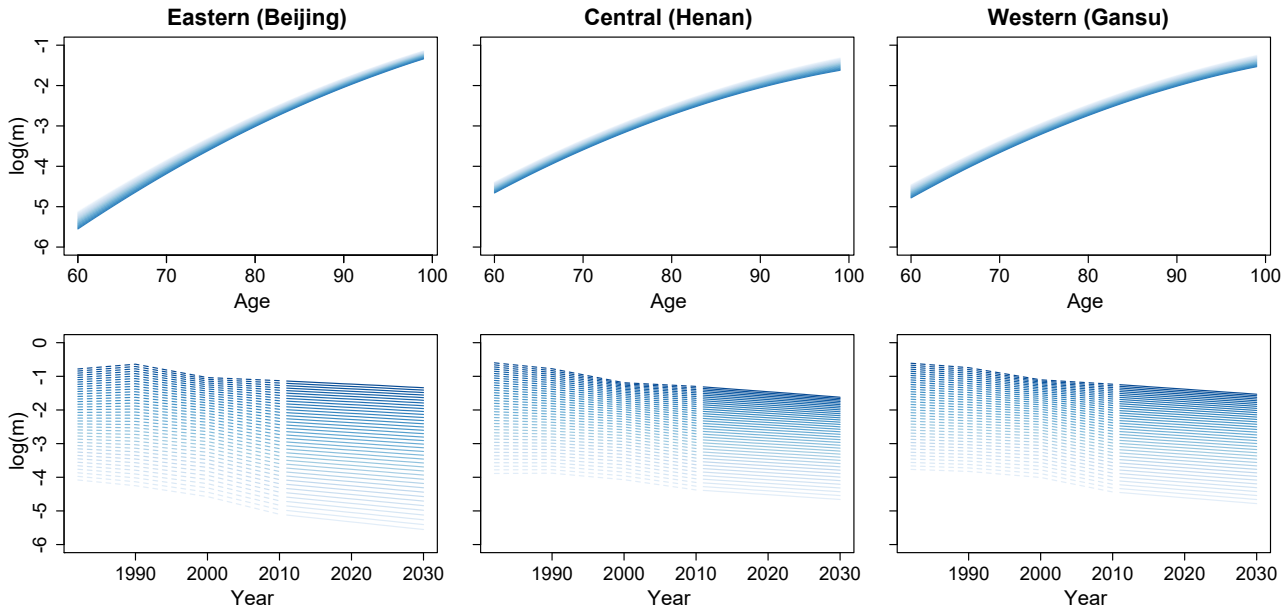

Figure 12. Median forecasts of $log(m^i_{x,t})$ for M1 during 2011–2030

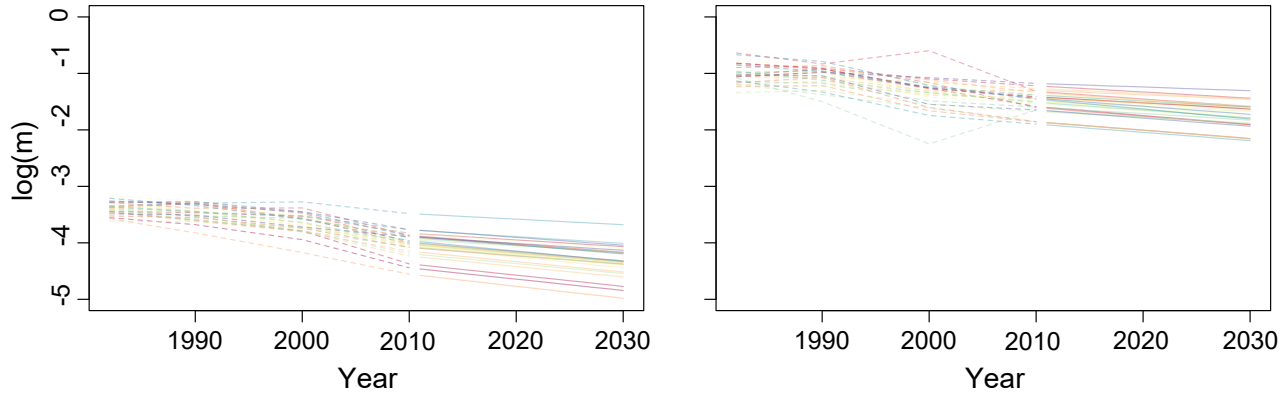

Figure 13. Median forecasts of $log(m^i_{x,t})$ for M1 at ages 65 and 95 for all provinces

age. The fitted mortality in 2000 is higher than that in 1982 and 1990, especially for older ages. As the common factors and reporting probability maintain a plausible age curvature, despite the data errors, M1 gives stable and plausible forecasts along the age dimension (Figure 14(a)). Although the mortality rates of Shanxi in 2000 have higher estimations than in the other years, as shown in Figure 14(b), M1 generates plausible forecasts along the year dimension.

5.2. Mortality forecast intervals

Figure 15 shows the medians and 95% fitting and forecasting intervals based on M1 for ages 65 and 95. The black solid and dashed lines are the medians and 95% intervals at age 65, while the grey solid and dashed lines are the medians and 95% intervals at age 95, respectively. Overall, the fitting and forecasting intervals are a little wider at age 95 than at age 65, reflecting the bigger historical uncertainty at higher ages. The forecasts are coherent between ages, as shown in Figure 15.

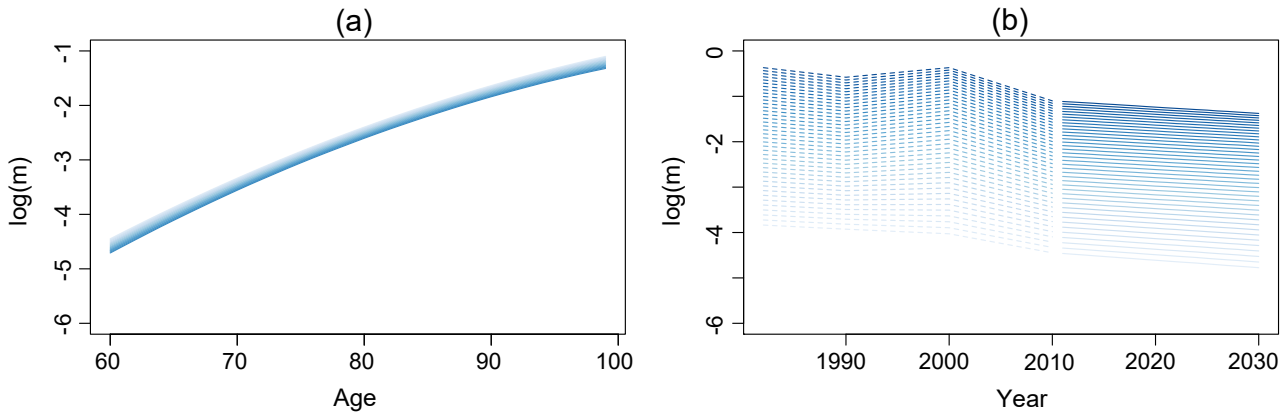

Figure 14. Median forecasts for Shanxi Province

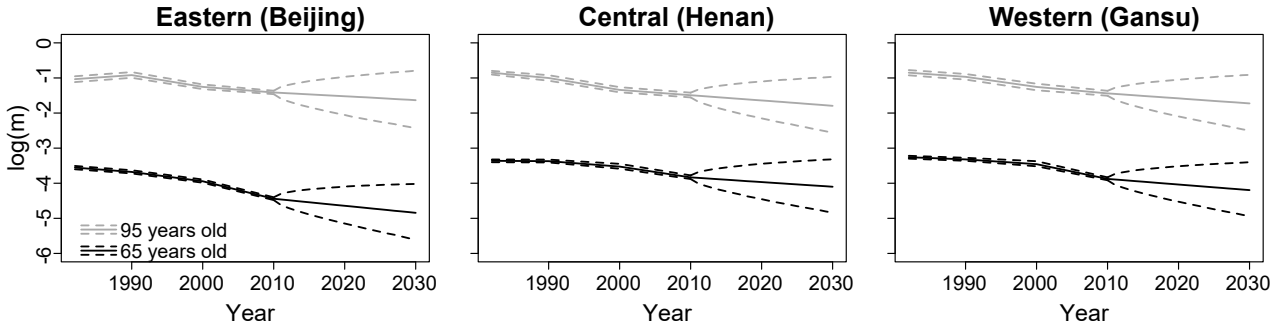

Figure 15. Median mortality fit, forecasts, and 95% intervals for ages 65 and 95 based on M1

In summary, model M2 gives larger age curvatures in the forecasts and lower projections at younger and advanced ages than model M1. The age curvature for M2 increases with the years of forecasting; thus, forecasting without the reporting probability may generate spurious projections. By contrast, model M1, which accounts for the reporting probability, gives plausible and coherent forecasts despite data errors.

5.3. Forecasts of life expectancy

Figure 16 shows the life expectancy ranks at age 60 (LE_{60}) and 95 (LE_{95}) in 2030. The dark grey lines and grey shaded areas show the medians and the 95% posterior intervals for M1 and the black lines and dashed lines the estimated medians and the corresponding 95% posterior intervals for M2, respectively. The provinces are ranked by LE_{60}. Overall, M2 has higher median LE_{60} and LE_{95}. Hainan Province, which is a southern island, has the longest LE_{60}. Based on the forecasts for M1, the median for LE_{60} varies from 20.23 to 25.97 years, being shown as the map of LE_{60} in Figure 17, while it varies from 20.52 to 26.71 years based on the forecasts for M2. The ranks of LE_{95} are different from age 60. The median of LE_{95} varies from 3.27 to 8.51 years based on M1. M2 generates much longer median LE_{95} and wider intervals at age 95, with LE_{95} varying from 4.44 to 12.68 years. Although Tibet has a shorter

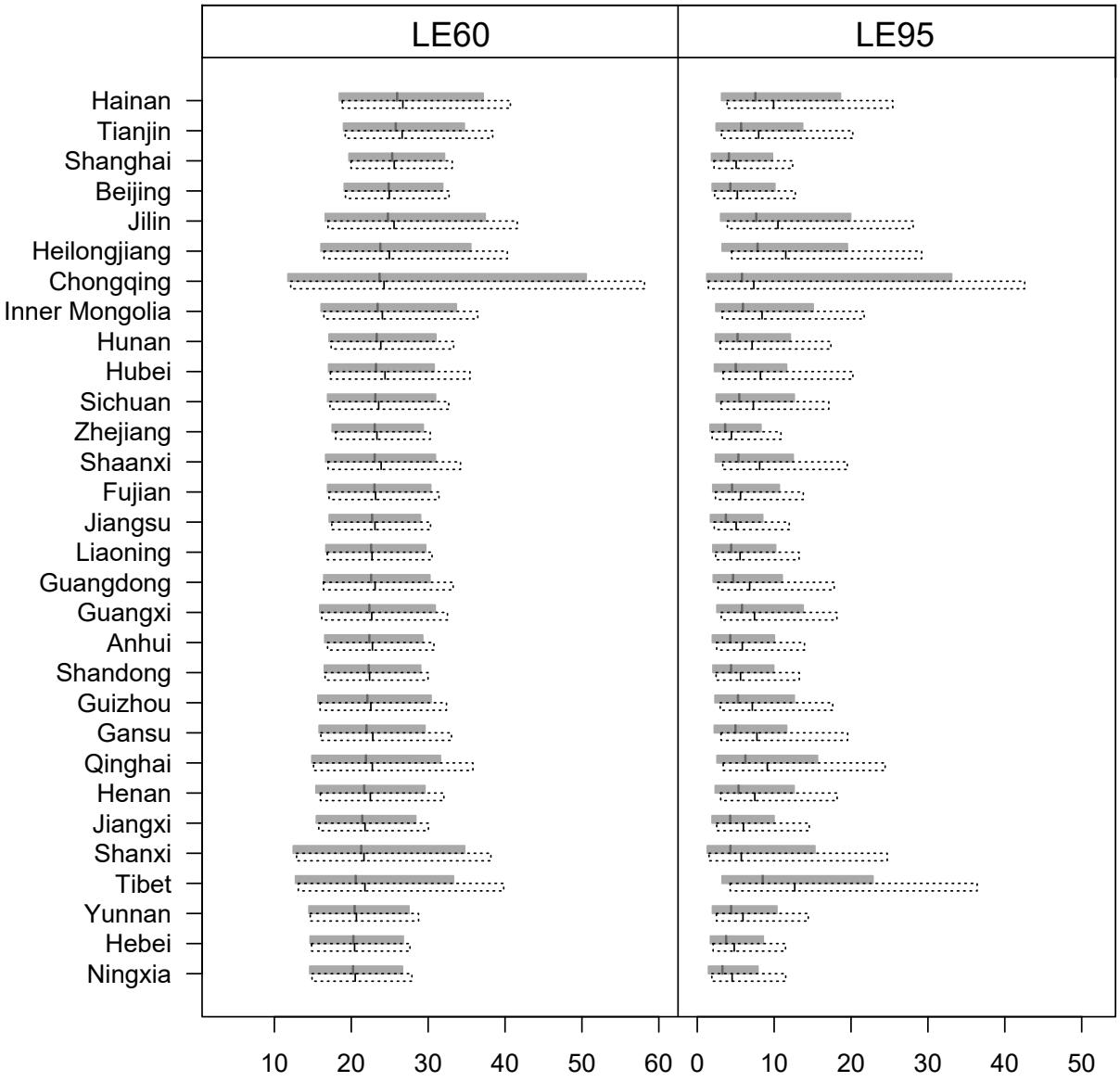

Figure 16. Forecasts of LE_{60} and LE_{95} in 2030

LE_{60} compared to the other provinces, it has the longest LE_{95}. Chongqing Province has much wider intervals than other provinces because the data are only available from 2000 onward, which indicates that missing data will lead to larger uncertainties in the projection.

6. Conclusions

In this paper, we propose a general mortality model for subnational populations at advanced ages. The model corrects for incomplete death reporting using a reporting probability under a Bayesian framework. We apply the model to fit and project provincial mortality in China for the age range 60–99. The proposed model has a better fit and a lower DIC than a similar model without the reporting probability. It can also deal with missing data, and the fitting intervals reflect historical uncertainty. Our model also performs well in terms of projections

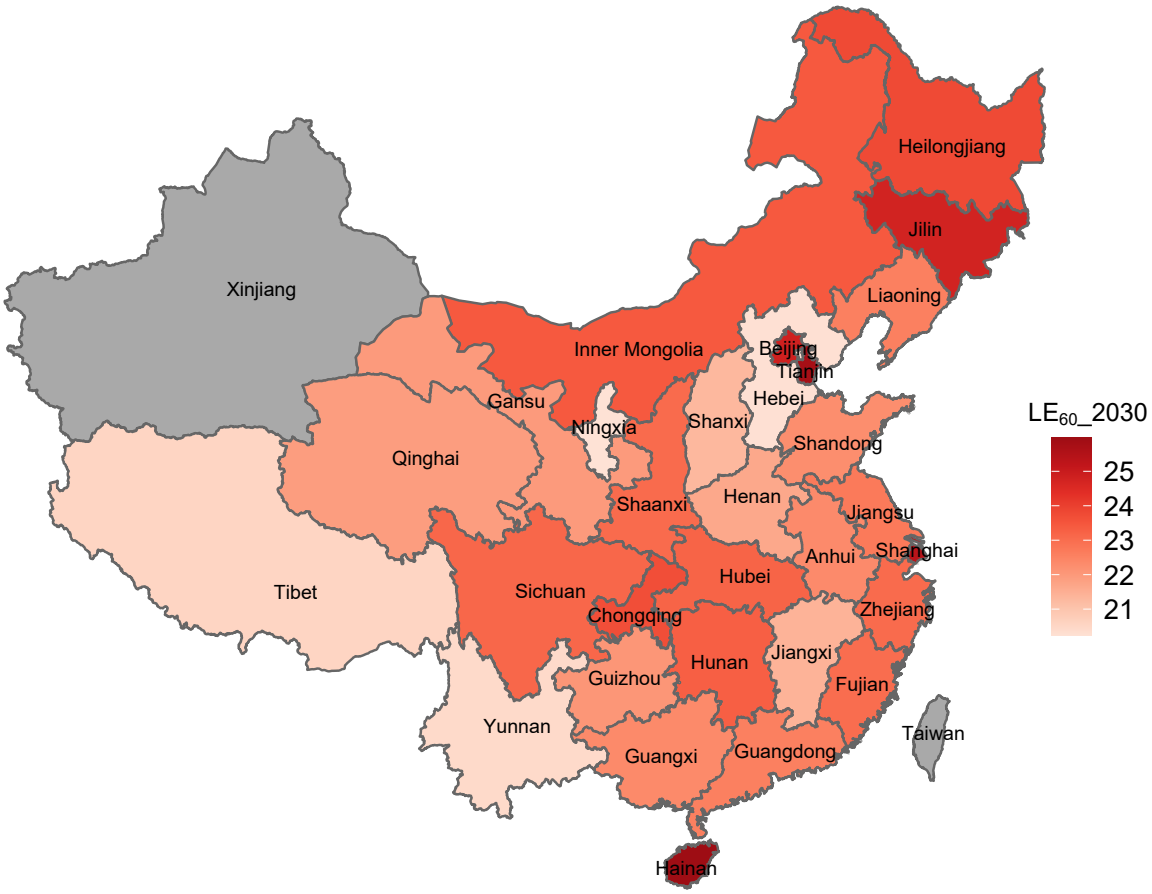

Figure 17. Map of provincial LE_{60} for model M1 in 2030 (grey areas mean no available data)

and generates coherent and plausible forecasts. Moreover, it provides age-specific estimates of the reporting probability by a single year of age. With the reporting probability, the estimated mortality curves have reasonable age curvatures even when the data are volatile or incomplete. However, without the reporting probability, the missing and underreported data dominate the mortality curves at higher ages, leading to unusual age curvatures and underestimation of the real mortality.

Our results show mortality can be modeled when high-quality data are unavailable, as the reporting probability can correct the underreported mortality and is useful in countries where registration or census mortality data are incomplete or underreported. Our model can be readily applied to these countries. Furthermore, even in developed countries with high-quality data, mortality data at advanced ages can suffer from missing or sparse observations. The proposed model can also be used in this case. Therefore, given its ability to deal with underreported data, its simple form, high efficiency (fit and forecasts in one stage), and good performance, our model is also recommended to developed countries.

There are two possible limitations of the proposed model. First, the model needs assumptions on the underreporting level of the reference year. We make assumptions based on previous

studies. If no such information is available, the assumption on the first-year coverage should be chosen with caution. Second, our model uses registered data. Systematic errors in registered data (e.g., low mortality rates reported for Shanxi Province in 2000) will lead to spurious estimates. Nevertheless, the model can deal with errors in the data and generate plausible forecasts. Overall, despite these limitations, the model works well when high-quality data are unavailable.

The proposed model extends the CBD family of models (Cairns et al., 2006), which was designed for older age mortality (age 60 and older). However, the problem of incomplete deaths can exist for all ages, and our model is not constrained to a specific model family. Further research can develop models for other ages or all ages based on other mortality models, such as the Lee-Carter model (Lee and Carter, 1992). Future research can also simultaneously consider incomplete population and death reporting.

Acknowledgement

This research was supported by the Australian Research Council Centre of Excellence in Population Ageing Research (project number CE170100005).

References

Alexander, M., Zagheni, E., & Barbieri, M. (2017). A flexible Bayesian model for estimating subnational mortality. *Demography*, 54 (6), 2025-2041.

Banister, J., Hill, K., 2004. Mortality in China 1964–2000. *Population Studies*, 58, 55–75.

Cairns, A. J., Blake, D., & Dowd, K. (2006). A two-factor model for stochastic mortality with parameter uncertainty: Theory and calibration. *Journal of Risk and Insurance*, 73(4), 687-718.

Cairns, A. J., Blake, D., Dowd, K., Coughlan, G. D., Epstein, D., Ong, A., & Balevich, I. (2009). A quantitative comparison of stochastic mortality models using data from England and Wales and the United States. *North American Actuarial Journal*, 13(1), 1-35.

Cairns, A. J., Blake, D., Dowd, K., & Kessler, A. R. (2016). Phantoms never die: Living with unreliable population data. *Journal of the Royal Statistical Society: Series A (Statistics in Society)*, 179(4), 975-1005.

Chan, W. S., Li, J. S. H., & Li, J. (2014). The CBD mortality indexes: Modeling and applications. *North American Actuarial Journal*, 18(1), 38-58.

Coale, A. J., Demeny, P., & Vaughan, B. (1983). *Regional Model Life Tables and Stable Populations: Studies in Population.* 2nd edition. New York, NY: Academic Press.

Coale, A. J. (1984). Rapid Population Change in China, 1952–1982. Committee on Population and Demography, *Report No. 27*. Washington, DC: National Academy Press.

Coale, A. J., & Banister, J. (1994). Five decades of missing females in China. *Demography*, 31 (3): 459–479.

Coale, A. J., & Li, S. (1991). The effect of age misreporting in China on the calculation of mortality rates at very high ages. *Demography*, 28(2), 293-301.

Cui H., Xu L., Li R. (2013). An Evaluation of Data Accuracy of the 2010 Population Census of China. *Population Research*, 37(1), 10-21. (in Chinese)

Currie, I. D. (2011). Modelling and forecasting the mortality of the very old. *ASTIN Bulletin: The Journal of the IAA*, 41(2), 419-427.

Dowd, K., & Blake, D. (2019). On the Projection of Mortality Rates to Extreme Old Age. *PI-1909*. London, UK: Pensions Institute.

Gale, W. G., & Krupkin, A. (2016). Financing State and Local Pension Obligations: Issues and Options. *Brookings Report*. Retirement Security Project, Brookings Institution, July 19. https://www.brookings.edu/research/financing-state-andlocal-pension-obligations-issues-and-options/.

Gavrilov, L. A., Gavrilova, N. S., & Krut'ko, V. N. (2017). Historical Evolution of Old-Age Mortality and New Approaches to Mortality Forecasting. *Living to 100 Monograph*, 2017(1B).

Gavrilov, L. A., & Gavrilova, N. S. (2019a). Late-life mortality is underestimated because of data errors. *PLoS Biology*, 17(2), e3000148.

Gavrilov, L. A., & Gavrilova, N. S. (2019b). New Trend in Old-Age Mortality: Gompertzialization of Mortality Trajectory. *Gerontology*, 65(5), 451-457.

Glen, A. G., & Leemis, L. M. (Eds.). (2017). International series in operations research & management science. *Computational probability applications*. Cham, Switzerland: Springer.

Hill, K., You, D.,& Choi, Y. (2009). Death distribution methods for estimating adult mortality: Sensitivity analysis with simulated data errors. *Demographic Research*, 21, 235-254.

Hunt, A., & Blake, D. (2014). A General Procedure for Constructing Mortality Models. *North American Actuarial Journal*, 18:1, 116-138.

Hunt, A., & Blake, D. (2020). Identifiability in Age/Period Mortality Models. *Annals of Actuarial Science*, forthcoming.

Khana, D., Rossen, L.M., Hedegaard, H., & Warner, M. (2018). A Bayesian spatial and temporal modeling approach to mapping geographic variation in mortality rates for subnational areas with R-INLA. *Journal of Data Science*, 16 (1), 147.

Leknes, S., & Løkken, S. A. (2020). *Empirical Bayes estimation of local demographic rates. An application using Norwegian registry data.* Statistics Norway.

Li, S. (1994). Levels and Patterns of Mortality in the 1980s in China. *Population Research*, 3: 37-44. (in Chinese)

Li, J. S. H., Zhou, R., & Hardy, M. (2015). A step-by-step guide to building two-population stochastic mortality models. *Insurance: Mathematics and Economics*, 63, 121-134.

Li, H., & O'Hare, C. (2017). Semi-parametric extensions of the Cairns–Blake–Dowd model: A one-dimensional kernel smoothing approach. *Insurance: Mathematics and Economics*, 77, 166-176.

Li, J., & Liu, J. (2019). A logistic two-population mortality projection model for modelling mortality at advanced ages for both sexes. *Scandinavian Actuarial Journal*, 2019(2), 97-112.

Lu, Q., Hanewald, K., & Wang, X. (2019). Bayesian Hierarchical Multi-Population Mortality Modelling for China's Provinces. *ARC Centre of Excellence in Population Ageing Research (CEPAR) Working Paper No. 2019/17.*

Ma, X., Duan, C., & Guo, J. (2014). A comparative study of the four types of migration. *Population Journal*, 5, 36-46. (in Chinese)

Office for National Statistics. (2019). Life expectancy at birth and at age 65 years by local areas, UK. https://www.ons.gov.uk/peoplepopulationandcommunity/healthandsocialcare/healthandlifeexpectancies/datasets/lifeexpectancyatbirthandatage65bylocalareasuk.

Peralta, A., Benach, J., Espinel-Flores, V., Gotsens, M., Borrell, C., & Marí-Dell'Olmo, M. (2020). Studying geographic inequalities in mortality in contexts with deficient data sources: Lessons from Ecuador. *Epidemiology*, 31(2), 290-300.

Permanyer, I., & Scholl, N. (2019). Global trends in lifespan inequality: 1950-2015. *PloS One*, 14(5).

Plummer, M. (2017). JAGS: Just another Gibbs sampler (Version 4.3.0)[Software].

Plummer, M. (2019). rjags: Bayesian Graphical Models using MCMC. R package version 4-10. https://CRAN.R-project.org/package=rjags.

Preston, S., Heuveline, P., & Guillot, M. (2000). *Demography: Measuring and Modeling Population Processes.* Wiley-Blackwell, Malden, MA.

Queiroz B. L., Freire F. H. M. A., Gonzaga M. R., & Lima E. E. C. (2017). Completeness of death-count coverage and adult mortality (45q15) for Brazilian states from 1980 to 2010. *Brazilian Journal of Epidemiology*, 20 (01), 21.

R Core Team (2020). R: A language and environment for statistical computing. R Foundation

for Statistical Computing, Vienna, Austria. URL https://www.R-project.org/.

Riffe, T., Lima, E., & Queiroz, B. (2017). DDM: Death Registration Coverage Estimation. R package version 1.0-0. https://CRAN.R-project.org/package=DDM.

Schmertmann, C. P., & Gonzaga, M. R. (2018). Bayesian estimation of age-specific mortality and life expectancy for small areas with defective vital records. *Demography*, 55(4), 1363-1388.

Sun, F., Li, S., & Li, N. (1993). Death Under-reporting in the Fourth Census in China and Some Provinces. *Chinese Journal of Population Science*, 2: 20-25. (in Chinese)

United Nations, Department of Economic and Social Affairs, Population Division (2019). *World Population Prospects: The 2019 Revision*, DVD Edition.

Wang, J. (2003). The 2005 China Population Census Missed Report Assessment and Mid-Year Population Estimate. *Population Research*, 27(5), 53-62. (in Chinese)

Wang, J., & Ge, Y. (2013). Assessment of 2010 Census Data Quality and Past Population Changes. *Population Research*, 37 (1), 22-33. (in Chinese)

Yan, H., Peters, G., & Chan, J. (2018). Mortality models incorporating long memory improves life table estimation: A comprehensive analysis. Working paper available at SSRN: https://ssrn.com/abstract=3149914.

Zhai Z. (1989). Levels and Patterns of Mortality in China from 1981 to 1987. *Population Journal*, 2: 12-18. (in Chinese)

Zou, X., & Wu, D. (2013). Floating population impact on Rural aging. *Population Journal*, 4, 70-79. (in Chinese)

Appendix

The posterior medians of real mortality $\log(m^i_{x,t})$ and registered mortality $\log(r^i_{x,t})$ for ages 60–99 for all provinces in 1982 are shown in Figures A1 and A2.

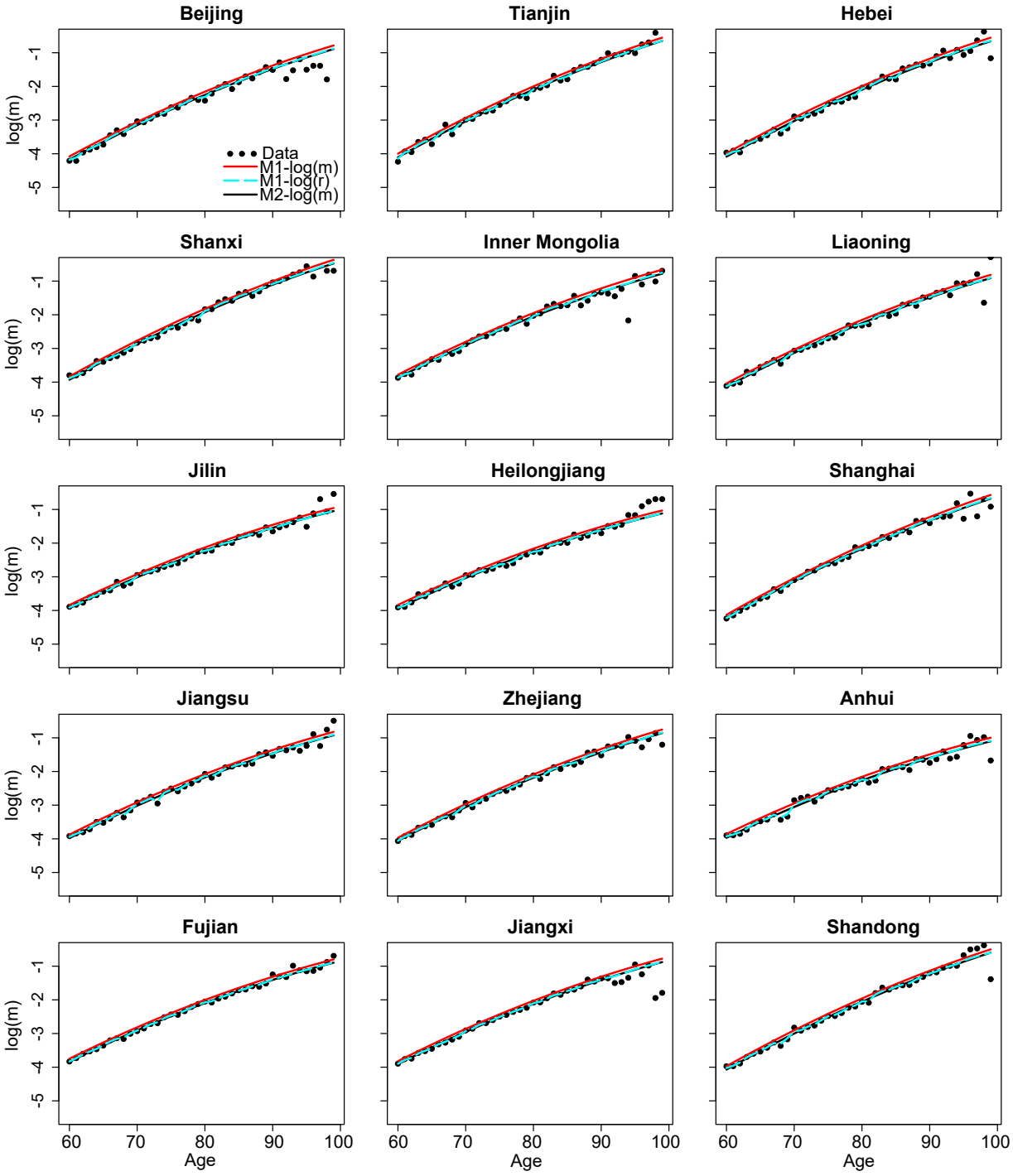

Figure A1. Posterior medians of real and registered mortality in 1982

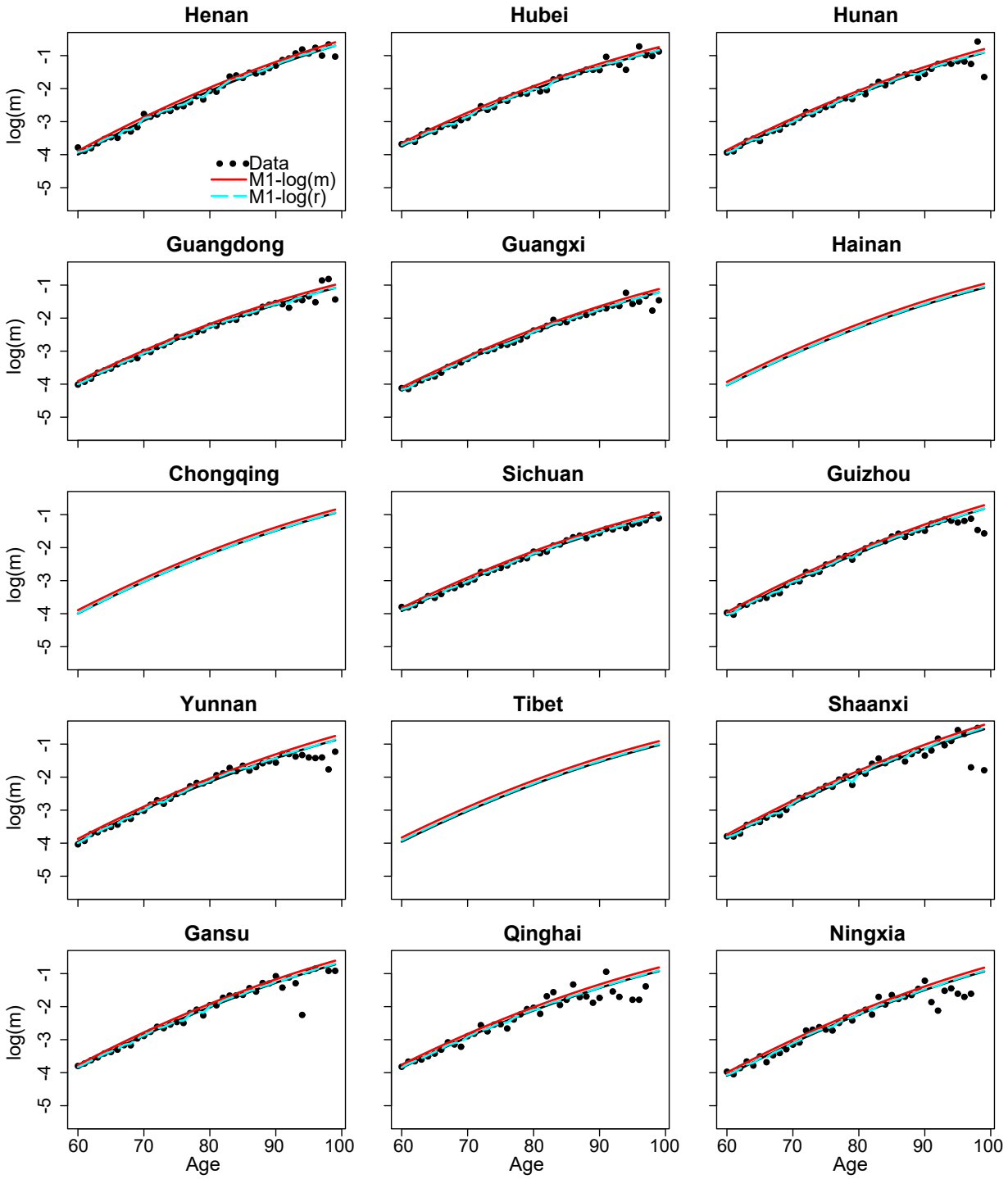

Figure A2. Posterior medians of real and registered mortality in 1982 (continued)

The posterior medians of real mortality $\log(m^i_{x,t})$ and registered mortality $\log(r^i_{x,t})$ for ages 60–99 in all provinces in 2010 are shown in Figures A3 and A4.

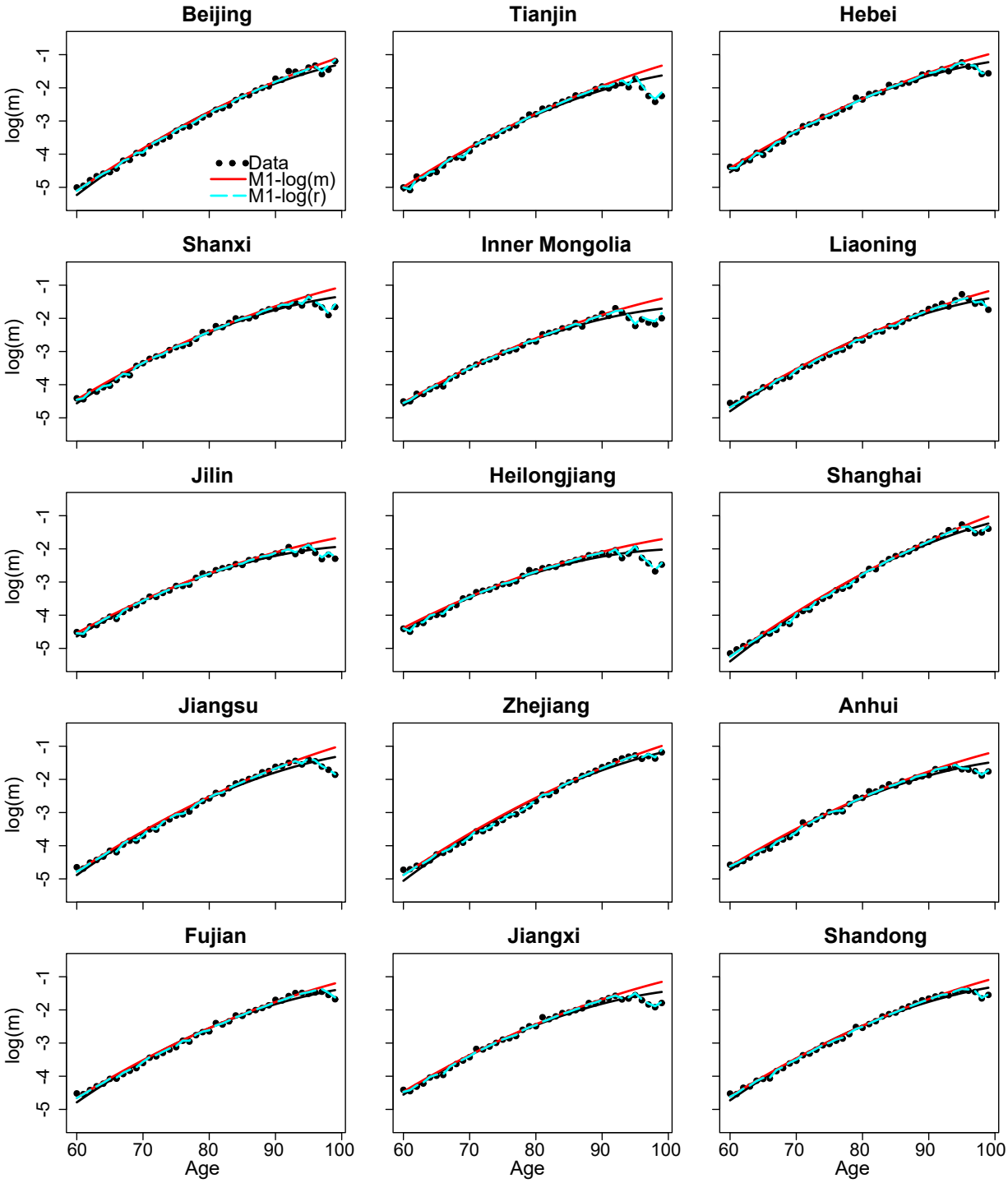

Figure A3. Posterior medians of real and registered mortality in 2010

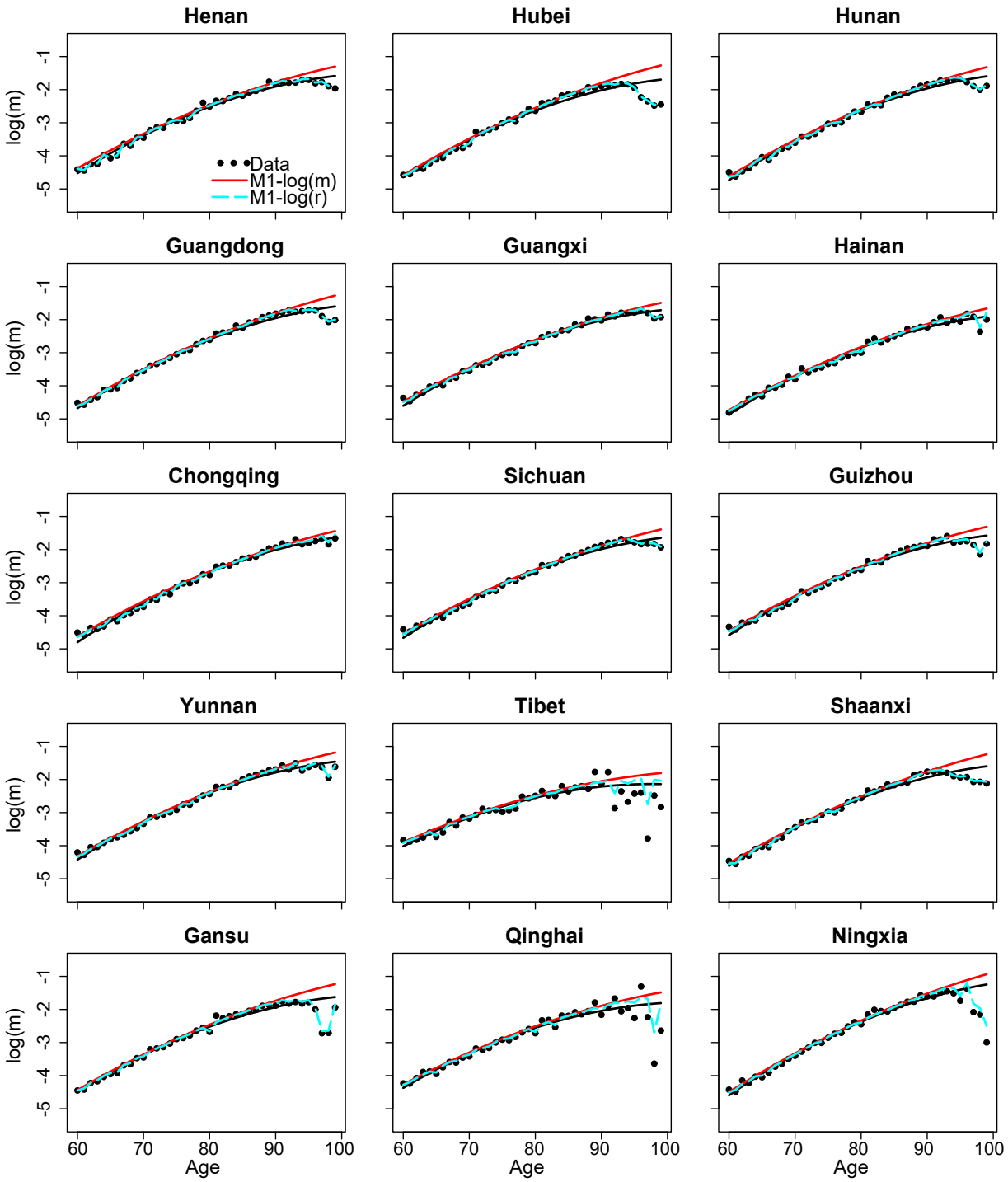

Figure A4. Posterior medians of real and registered mortality in 2010 (continued)

The posterior 95% intervals of real mortality $\log(m^i_{x,t})$ based on M1 for all provinces in 1982 are shown in Figures A5 and A6.

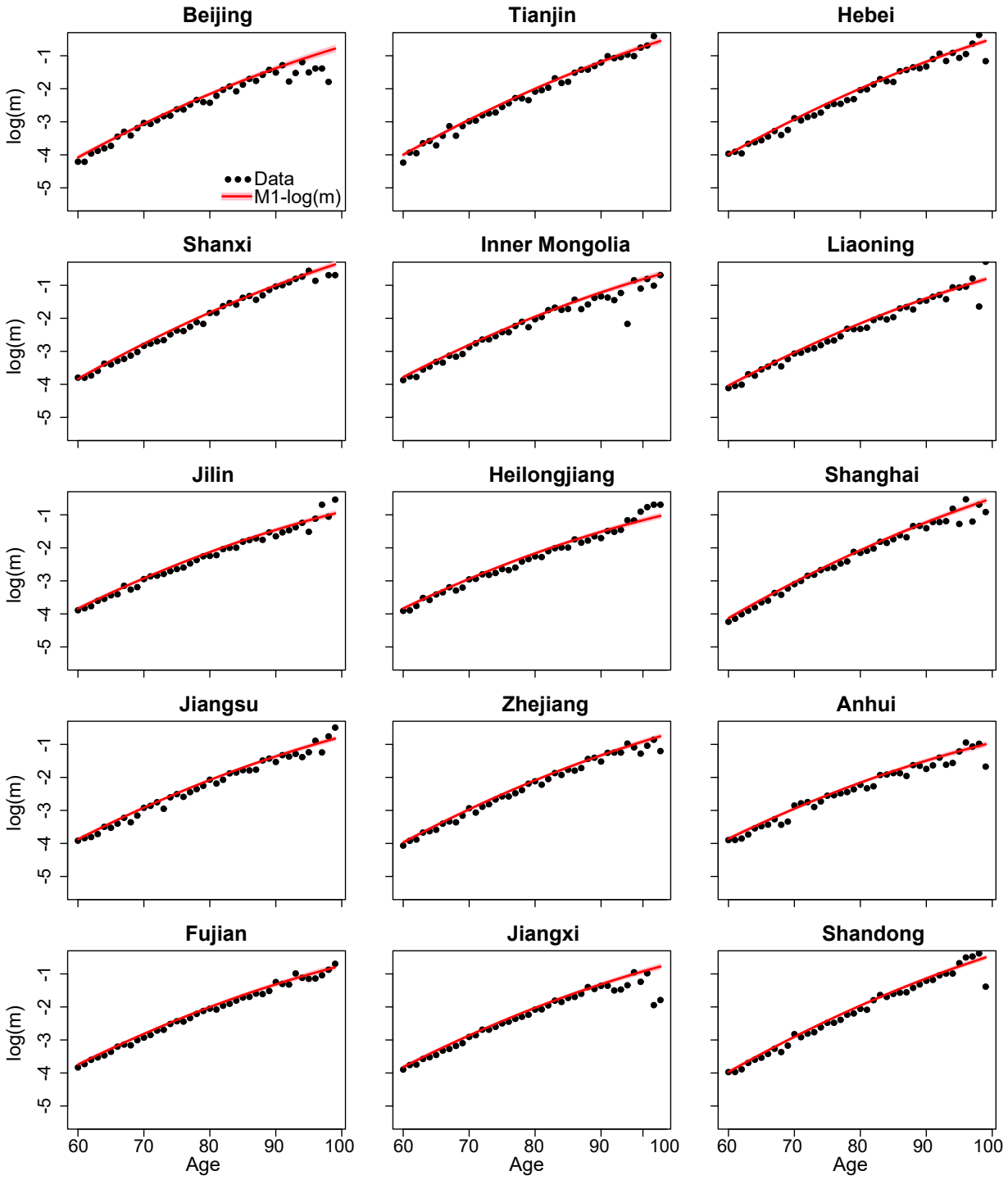

Figure A5. Posterior 95% intervals of real mortality based on M1 in 1982

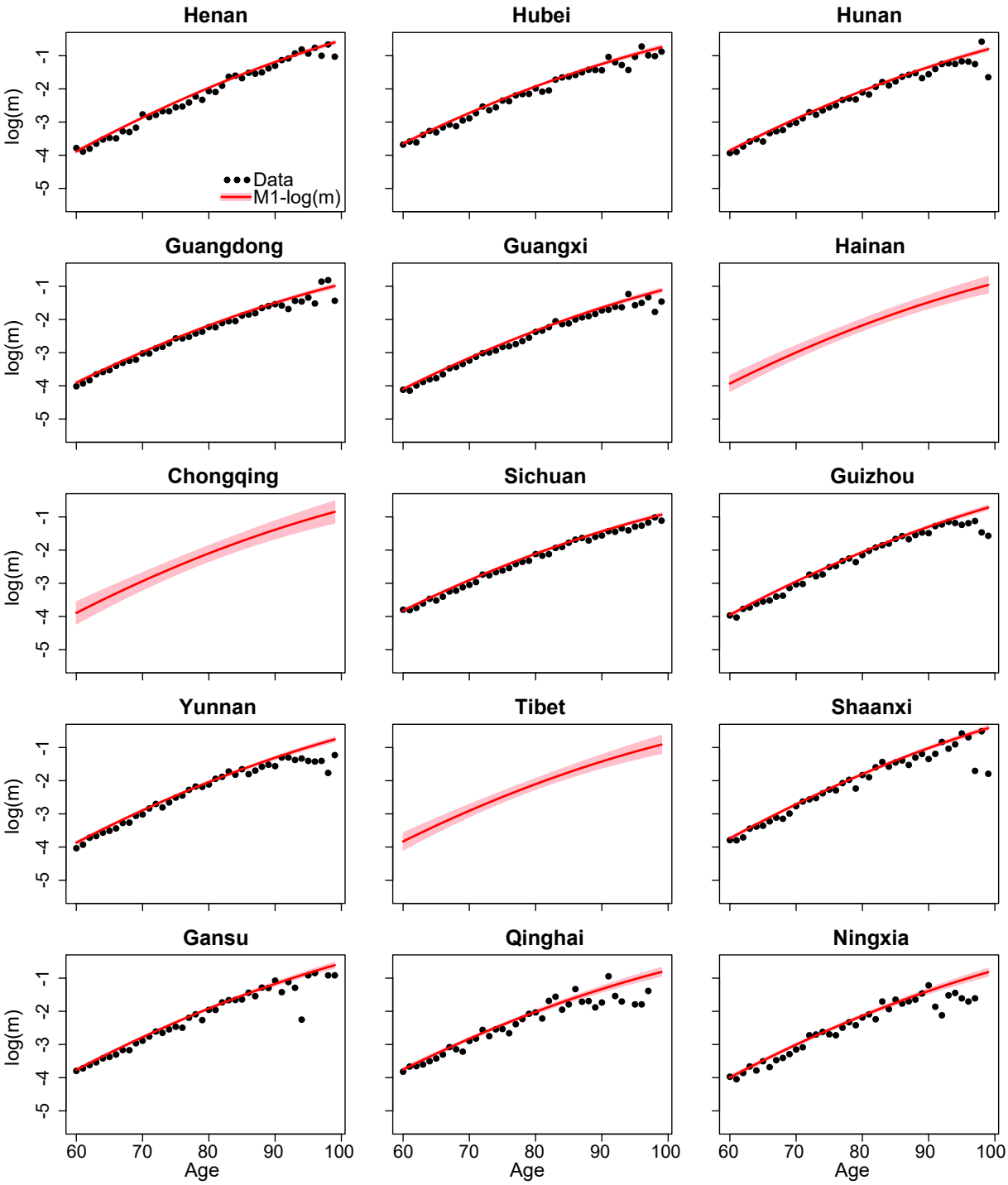

Figure A6. Posterior 95% intervals of real mortality based on M1 in 1982 (continued)

The posterior 95% intervals of real mortality $\log(m^i_{x,t})$ based on M1 for all provinces in 2010 are shown in Figures A7 and A8.

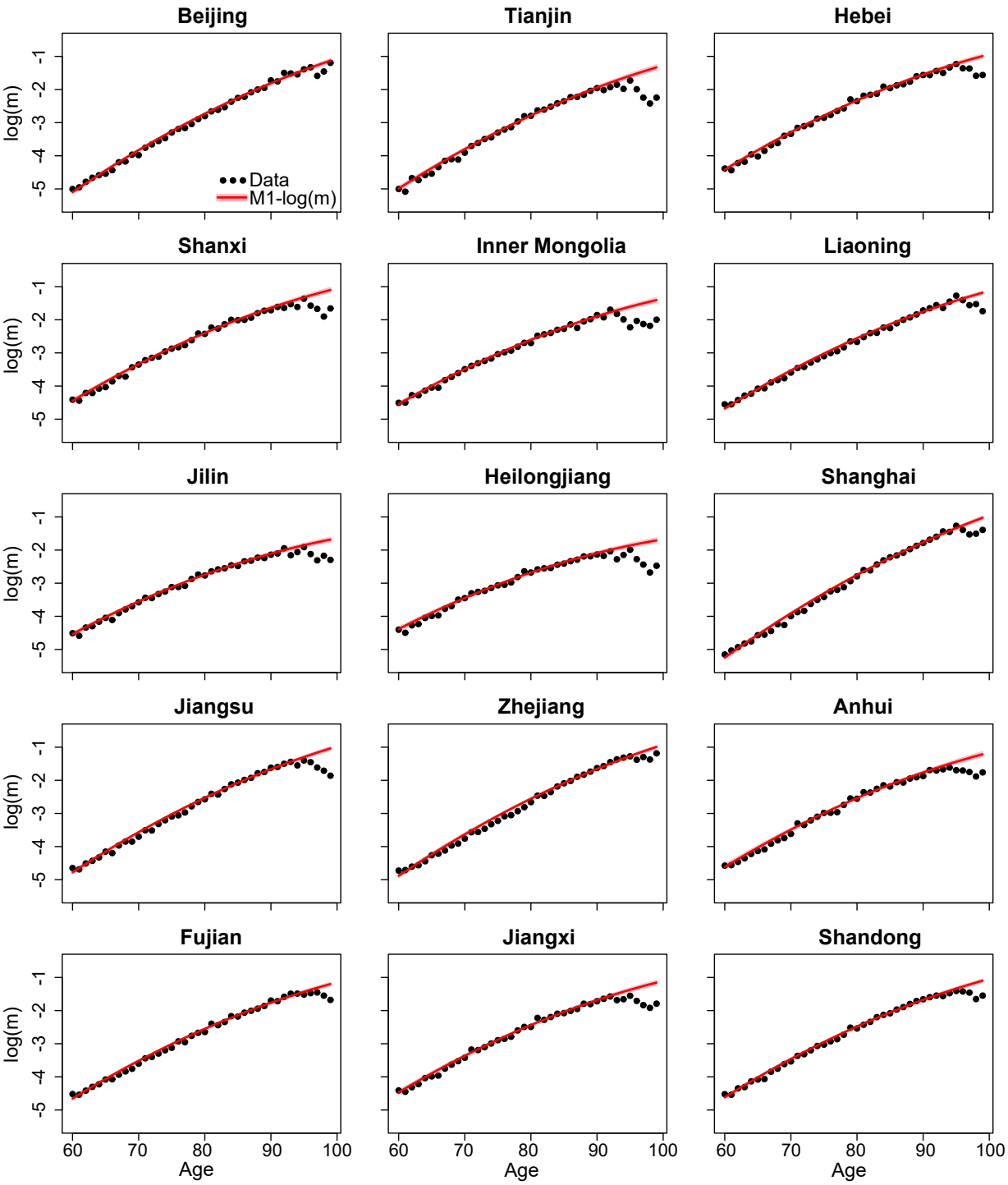

Figure A7. Posterior 95% intervals of real mortality based on M1 in 2010

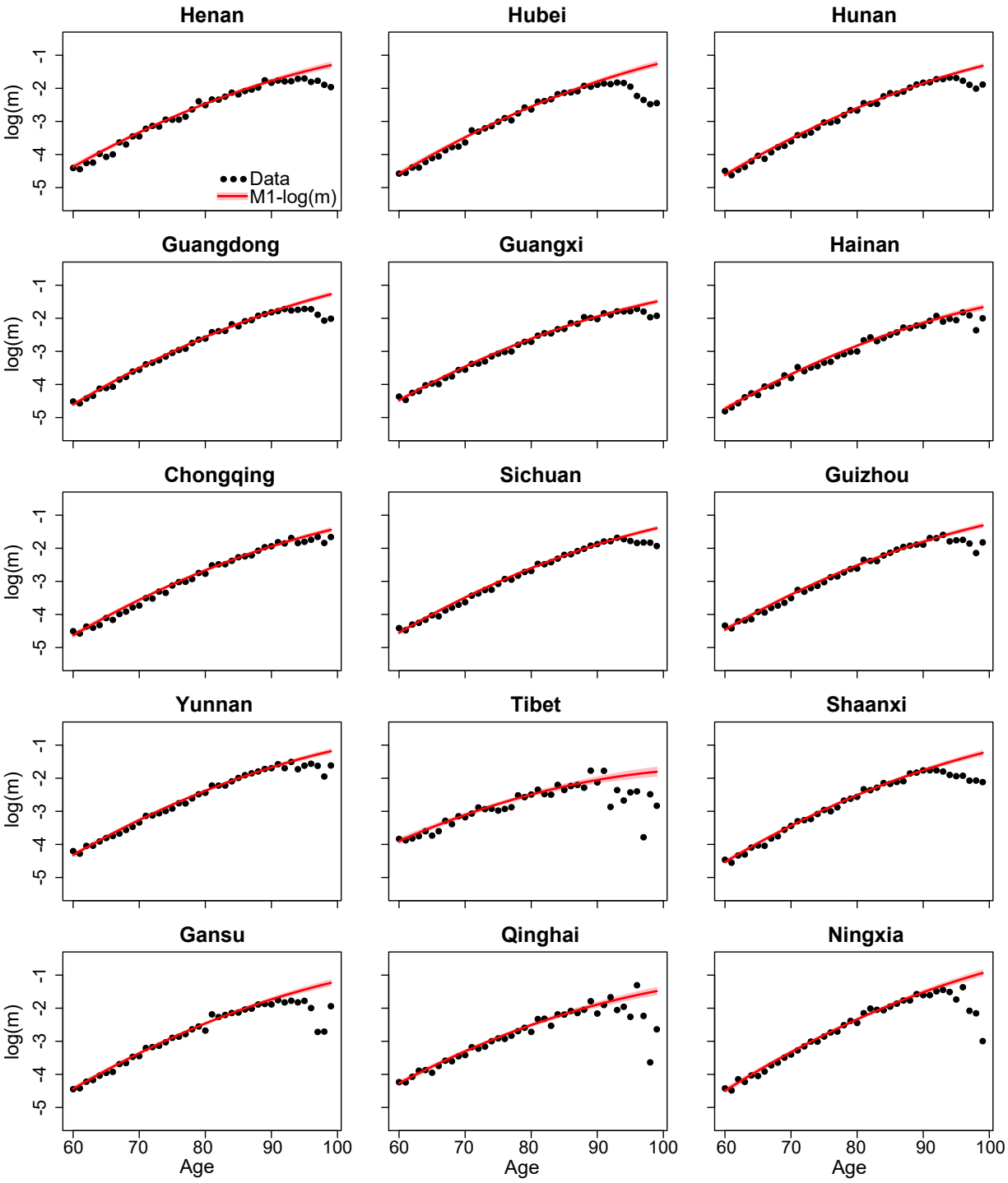

Figure A8. Posterior 95% intervals of real mortality based on M1 in 2010 (continued)

The median forecasts of real mortality $\log(m^i_{x,t})$ for all provinces are shown in Figures A9 and A10.

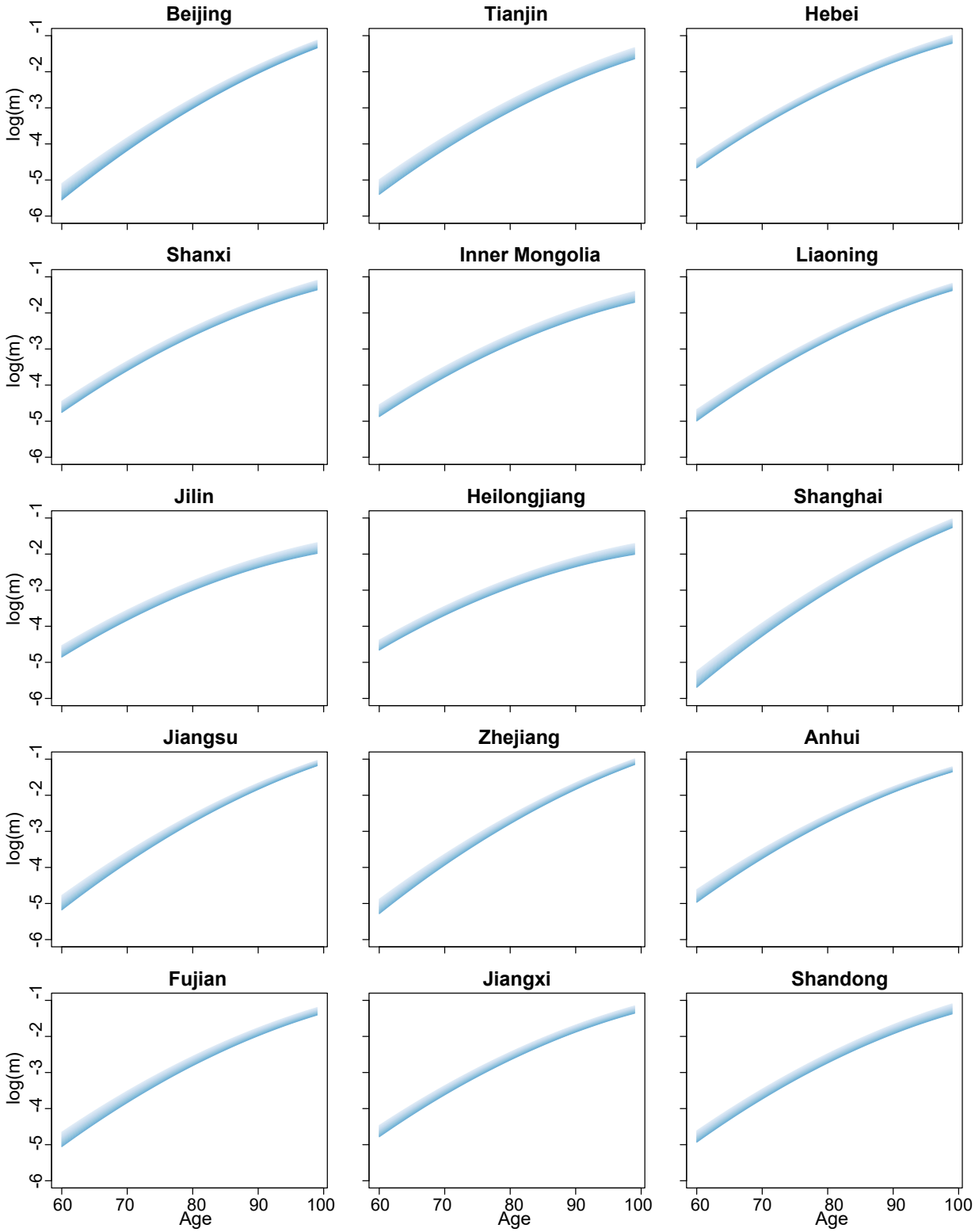

Figure A9. Median forecasts of real mortality

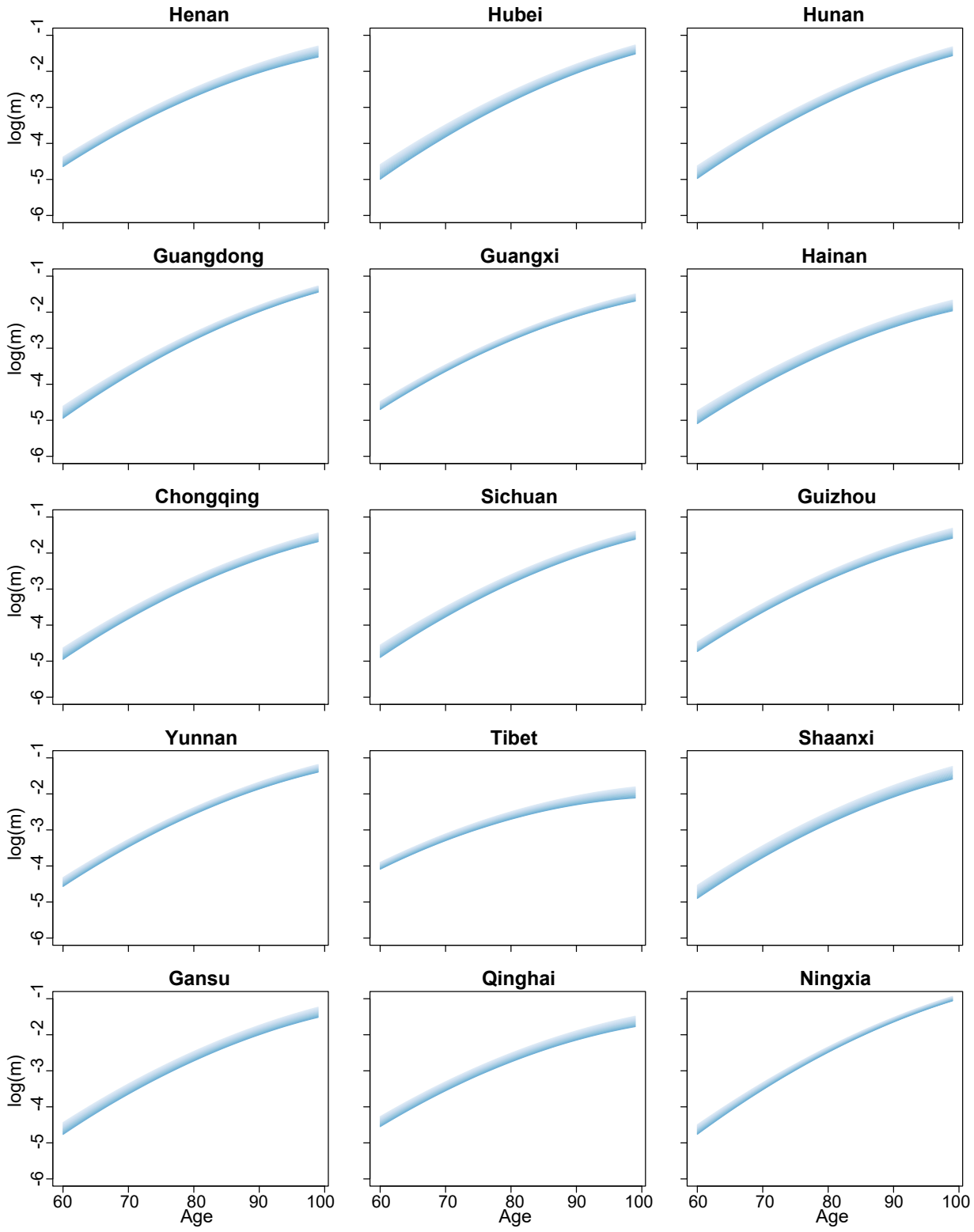

Figure A10. Median forecasts of real mortality (continued)